


RESEARCH ARTICLE OPEN ACCESS

Leukocyte and Lymphoid Organ Ontogeny

Survival and Developmental Progression of Unselected Thymocytes in the Absence of the T-Cell Adaptor Gads

Rose Shalah | Manal Marzouk | Enas Hallumi | Naama Klopstock | Deborah Yablonski 

Technion—Israel Institute of Technology, Rappaport Faculty of Medicine, Haifa, Israel

Correspondence: Deborah Yablonski (debya@technion.ac.il)**Received:** 9 January 2024 | **Revised:** 2 February 2025 | **Accepted:** 3 February 2025**Funding:** This research was supported by the Israel Science Foundation (283/22), the Rappaport Family Institute for Research in the Medical Sciences, the Minerva Stiftung Center Programme on Cell Intelligence, and the Colleck Research Fund.**Keywords:** TCR signaling | thymic development | adaptor proteins | death by neglect

ABSTRACT

Thymocyte β -selection and positive-selection depend on TCR signaling via the immune adaptors SLP-76 and LAT. Gads bridges the recruitment of SLP-76 to LAT, yet is not required for the maturation of single positive (SP) thymocytes. To illuminate this paradox, we performed tamoxifen-induced ablation of Gads (Gads^{IKO}), accompanied by the expression of tdTomato, and compared the development of Gads-expressing (Tom⁻) and Gads-ablated (Tom⁺) thymocytes within the same mouse. Gads^{IKO} (Tom⁺) thymocytes exhibited impaired β - and positive-selection, yet δ -selection was not affected. While susceptible to apoptosis ex vivo, the marked accumulation of self-MHC nonresponding (CD5⁻) Gads^{IKO} DP thymocytes suggested the possibility of impaired death by neglect in situ. Further supporting this notion, Gads^{IKO} CD5^{lo} DP thymocytes exhibited reduced apoptosis in situ and reduced CD8-induced apoptosis ex vivo. Most Gads^{IKO} CD4 SP thymocytes were positively selected, yet a distinct population of unselected (CD5⁻ TCR β ^{neg/low} CCR7^{lo} CD24^{hi}) CD4 SP thymocytes was seen only in the absence of Gads. This unselected population did not include Treg or TCR $\gamma\delta$ subsets; rather, it encompassed CD44^{lo} CD25⁺ cells, resembling pre- β -selection thymocytes. Our results suggest that Gads promotes passage through key TCR-driven developmental checkpoints while repressing the progression of unselected DN and DP thymocytes.

1 | Introduction

At every stage of their life cycle, T cell development, differentiation, and function are tightly controlled by signaling through the clonotypic T cell antigen receptor (TCR). This principle is most clearly exemplified by thymocyte development, in which the strength of TCR signaling controls multiple developmental checkpoints [1–4].

Conventional thymocyte development proceeds through three main stages, known as double negative (DN, CD4⁻CD8⁻), double positive (DP, CD4⁺CD8⁺), and single positive (SP, either CD4⁺

or CD8⁺). The DN compartment is further divided into four substages, based on the expression of surface markers that define DN1 (CD44⁺CD25⁻), DN2 (CD44⁺CD25⁺), DN3 (CD44⁻CD25⁺), and DN4 (CD44⁻CD25⁻) [5].

As thymocytes pass through the DN compartment, productive rearrangement of TCR β is required for expression of the pre-TCR. Signals emanating from the pre-TCR trigger β -selection, which is characterized by rapid thymocyte proliferation and upregulation of CD5, along with the passage of DN3 thymocytes through DN4 and into the DP compartment [6–8]. In parallel, TCR $\gamma\delta$ rearrangement triggers roughly analogous events, known

Rose Shalah and Manal Marzouk contributed equally to the revision of this study.

This is an open access article under the terms of the [Creative Commons Attribution-NonCommercial-NoDerivs](https://creativecommons.org/licenses/by-nc-nd/4.0/) License, which permits use and distribution in any medium, provided the original work is properly cited, the use is non-commercial and no modifications or adaptations are made.

© 2025 The Author(s). *European Journal of Immunology* published by Wiley-VCH GmbH

as δ -selection, resulting in the differentiation of $\gamma\delta$ T cells [9, 10].

The mature $\alpha\beta$ TCR is first expressed during the DP stage, where its ability to recognize self-peptide-MHC (p-MHC) can be assessed by following activation markers, including CD69, CD5, and surface TCR β [8, 11–13]. Low expression of CD5 identifies DP cells that fail to recognize self-p-MHC [11]; these cells may be removed through a process called “death by neglect” [14, 15]. Evidence suggests that 80–90% of DP thymocytes may undergo death by neglect [14–16], yet the precise mechanisms triggering this process are still unknown. On the other hand, strong recognition of self-p-MHC triggers death by negative selection.

Between these two extremes, weak self-recognition triggers positive selection and transition to the SP compartments [17]. Positively selected SP cells transiently express CD69, moreover, they are typically TCR β^{hi} and CD5 $^{\text{hi}}$ and follow a maturation trajectory, during which expression of CCR7 transiently increases and CD24 decreases, prior to their exit from the thymus as naive peripheral T cells [13, 18, 19]. Taken together, the ability of T cells to correctly interpret the strength of TCR ligation profoundly shapes thymocyte development, eventually allowing T cells to distinguish between self and foreign antigens [1–4].

TCR ligation triggers a cascade of tyrosine kinases [20, 21], initiated by a Src-family kinase, Lck, which activates a Syk-family kinase, ZAP-70. ZAP-70 phosphorylates two adaptor proteins, LAT and SLP-76 [22–28], triggering the SH2-mediated binding of multiple signaling proteins to the adaptors (reviewed in [29, 30]).

Gads is an evolutionarily conserved, Grb2-family adaptor, expressed mainly in T cells and mast cells, and required for optimal antigen receptor signaling in these cell types [31]. Like Grb2, Gads consists of a central SH2 domain flanked by two SH3 domains but also includes a unique unstructured linker. Gads C-SH3 domain binds constitutively to SLP-76 [32–34], whereas its SH2 domain mediates the cooperative binding of Gads to two LAT phospho-sites, pY171 and pY191 [25, 33, 35]. Through these interactions, Gads bridges the TCR-induced recruitment of SLP-76 and its associated signaling proteins to phospho-LAT [36–40], where adaptor-associated enzymes trigger downstream responses [29, 31, 41]. Among the most important and best-understood downstream pathways, SLP-76-associated Itk phosphorylates LAT-associated PLC- γ 1, triggering the production of second messengers that increase intracellular calcium and activate the Ras-MAPK pathway.

Since the best-understood function of Gads is to bridge the TCR-induced recruitment of SLP-76 to LAT, it is surprising that germline deletion of these adaptors results in distinct phenotypes. Both SLP-76 and LAT are essential for thymocyte development beyond the DN3 stage [42–44]. In contrast, Gads-deficient mice exhibit incomplete blocks at multiple thymic checkpoints, associated with a marked reduction in thymic size.

Despite prominent impairment of β -selection, Gads is not required for the transition of DN thymocytes into the DP population [45]; indeed, germline Gads-deficient thymocytes progress through the DP compartment and into the SP compartments [46–48]. Moreover, the development of peripheral CD4 and CD8

T cell populations demonstrates that T cell development is at least partially Gads-independent [46, 47]. This paradox raises many questions about the mechanism by which potentially unselected or suboptimally selected cells may progress to and through the DP compartment [48]. One possibility that was not previously addressed is that Gads may be required for the apoptotic removal of unselected cells. Another possibility is that Gads may differentially affect different thymic populations [45]. Whereas previous studies on transgenic backgrounds support a role for Gads in positive selection [46, 48], this question has not been addressed on a diverse TCR background.

We hypothesized that Gads fine-tunes TCR responsiveness and thereby may affect multiple developmental checkpoints. To test our hypothesis, we established a genetic model that enabled us to compare the development of Gads-expressing and Gads-ablated thymocytes, side by side in the same mouse. This approach revealed multiple points at which Gads influences thymocyte development. Gads was required for efficient β -selection and optimal p-MHC-induced expression of CD69 and CD5, important correlates of positive selection. On the other hand, Gads was required for efficient death by neglect of MHC-nonresponsive DP thymocytes; in its absence, unselected, CD5 $^+$ thymocytes progressed as far as the CD4 SP compartment. This observation sheds light on the unexpected involvement of TCR signaling elements in the regulation of death by neglect.

2 | Results

2.1 | A Mouse Model for Inducible Deletion of Gads, Accompanied by the Expression of tdTomato

To better distinguish Gads-dependent and Gads-independent developmental pathways, we developed a mouse model system for the inducible deletion of Gads. This model is comprised of two “floxed” genes, Gads $^{\text{FL}}$ and Tom $^{\text{FL-stop}}$ (Figure 1A), both controlled by a ubiquitously-expressed tamoxifen-inducible Cre recombinase, UBC-Cre-ERT2 [50].

The Grap2 (Gads) gene comprises 7 coding exons, of which exons 1–2 encode the N-SH3 and exons 3–7 encode the SH2, linker, and C-SH3 domains [46]. Cre-mediated removal of Gads exon 2 creates a frameshift mutation that alters the protein sequence after K26, resulting in a premature stop codon that disrupts the N-SH3 and removes all downstream domains (Figure 1B).

2.2 | Prior to Cre-Mediated Ablation, Gads $^{\text{FL}}$ Supports Wild-Type Functionality

For initial validation of our model, we verified that prior to its Cre-mediated ablation, Gads $^{\text{FL}}$ supports wild type functionality. To this end, we compared thymic development in mice of three genotypes: Gads $^{+/+}$ (wild-type), Gads $^{\text{FL/FL}}$, and Gads $^{-/-}$ (germline Gads-deficient mice), while using a dump gate to exclude non-T cell lineages as well as NK1.1 $^+$ and TCR $\gamma\delta^+$ thymocytes.

Consistent with previous reports [46, 47], Gads $^{-/-}$ mice had markedly reduced thymic cellularity (Figure S1A), and an altered distribution of thymocyte subsets (Figure S1B–E). The partial

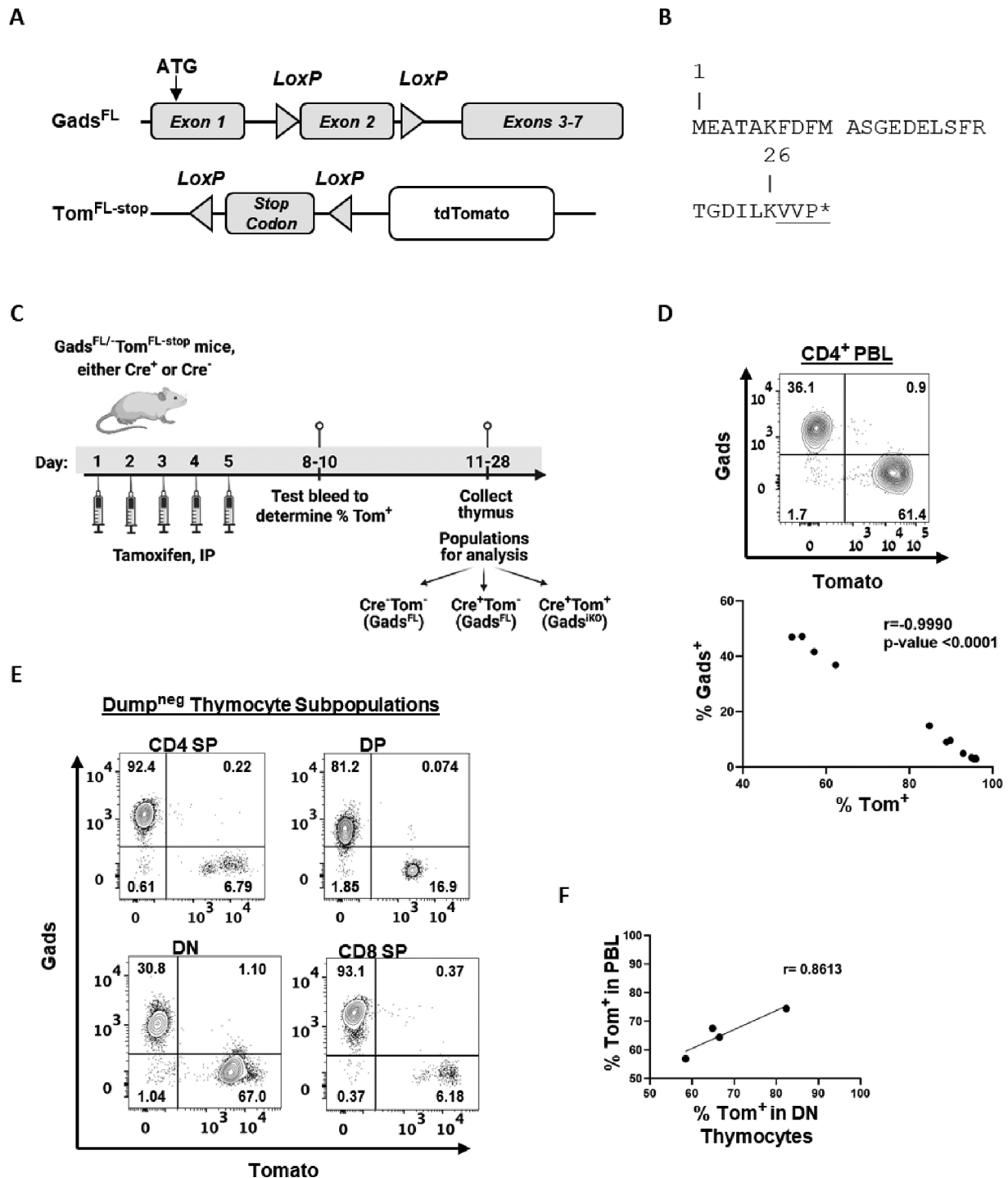


FIGURE 1 | A mouse model for inducible deletion of Gads, accompanied by the expression of tdTomato. The Gads^{IKO} mouse model comprises two “floxed” genes, whose expression is controlled by UBC-Cre-ERT2, a ubiquitously expressed tamoxifen-inducible Cre recombinase [50]. (A) Prior to Cre activity, LoxP sites flank exon 2 of *Grp2*, the gene that encodes Gads. Within the *Rosa26* locus, a second set of LoxP sites flank an in-frame stop codon that prevents the expression of a fluorescent marker, tdTomato [49]. (B) Cre-mediated recombination removes exon 2 of *Grp2*, creating a frameshift mutation that alters the protein sequence after K26 and results in a premature stop codon after 29 amino acids. (C) Experimental workflow for tamoxifen-inducible ablation of Gads. Created with BioRender.com. (D) One week after starting tamoxifen treatment, peripheral blood leukocytes (PBL) were stained for surface markers and intracellularly for Gads. Top: representative result for CD4⁺ T cells. Bottom: Frequency of Gads⁺ and Tom⁺ phenotypes in CD4⁺ peripheral blood T cells. $n = 13$ Cre⁺ mice. Pearson correlation coefficient (r) was calculated using Prism. (E) 3.5 weeks after starting tamoxifen treatment, thymocytes were stained for surface CD4 and CD8 and intracellularly for Gads. In this experiment, a mixture of FITC-labeled surface-staining antibodies (anti-mouse NK1.1, TER-119, Gr-1, CD11b, and B220) was employed to create a dump gate to exclude NK1.1⁺ thymocytes, as well as erythrocyte, granulocyte, macrophage, monocyte, and B cell lineages. A representative result is presented while gating on Dump^{neg} live (Zombie^{neg}) thymocytes. (F) Correlation between the frequency of Tom⁺ DN thymocytes and the frequency of Tom⁺ PBLs observed four days earlier in the same mice. Thymi were collected 2 weeks after starting tamoxifen.

block at the DN to DP transition was reflected in an increased frequency of DN thymocytes (Figure S1C) and a reduced frequency of DP and CD4 SP thymocytes (Figure S1D–E). Within the DN compartment, $Gads^{-/-}$ thymocytes exhibited the previously reported [46, 47] partial block at the DN3 to DN4 transition (Figure S1F), resulting in a markedly increased ratio of DN3 (CD44⁺ CD25⁺) to DN4 (CD44⁺ CD25⁻) cells (Figure S1G).

In all of these parameters, we observed statistically significant differences between $Gads$ -expressing and $Gads$ -deficient thymocytes, but no significant differences were observed between thymocytes expressing wild type and floxed $Gads$ (Figure S1A, C–E, G). This result was independent of the number of alleles of $Gads$ present; thus, $Gads^{FL/-}$ mice were not statistically different from $Gads^{+/-}$ mice, and both were statistically different from $Gads^{-/-}$ mice (data not shown). Together, these observations provide strong evidence that the LoxP sites surrounding $Gads$ exon 2 do not impair the expression or function of $Gads$.

2.3 | The tdTomato Marker Reliably Identifies $Gads^{iKO}$ Peripheral T Cells and Thymocytes

For inducible deletion of $Gads$, we administered tamoxifen for five consecutive days to UBC-Cre-ERT2⁺ $Gads^{FL/-}$ Tom^{FL-stop} mice; in parallel, we tamoxifen-treated an equal number of control Cre⁻ $Gads^{FL/-}$ Tom^{FL-stop} littermates (Figure 1C). We deliberately chose a genetic configuration in which one allele of $Gads$ is germline deleted and the other is floxed so that Cre-mediated recombination at a single floxed allele would suffice to render a cell $Gads$ -deficient ($Gads^{iKO}$). Concomitantly, Cre-mediated removal of the Tom^{FL-stop} in-frame stop codon renders the cell Tom⁺ [49]. By requiring only a single genetic change at each locus, this experimental design should promote maximal correlation between Tom expression and $Gads$ deficiency.

The use of a ubiquitous Cre construct allowed for the deletion of $Gads$ throughout the mouse, both in the thymus and in the periphery. Tom⁺ peripheral blood T cells were reproducibly observed 1 week after the initiation of tamoxifen treatment; however, their frequency varied between mice. The rapid appearance of Tom⁺ peripheral T cells suggests that they derive from Cre activity in pre-existing peripheral populations.

To more directly detect ablation of $Gads$, we stained PBLs intracellularly with a fluorescently-labeled anti- $Gads$ antibody and analyzed the results while gating on CD4⁺ or CD8⁺ T cells. Tom⁺ peripheral CD4⁺ and CD8⁺ T cells were uniformly $Gads$ -negative (Figure 1D, top and data not shown). A tight correlation between the Tom⁺ and $Gads^{iKO}$ phenotypes was apparent as soon as 1 week after the initiation of tamoxifen treatment (Figure 1D, bottom) and remained intact as long as 5 weeks after the initiation of tamoxifen treatment (data not shown).

To test whether Tom⁺ can likewise serve as a marker for $Gads$ -deficient thymocytes, we employed a dump gate to exclude non-T cell lineages, including NK1.1⁺ thymocytes, B cells, macrophages, dendritic cells, and red blood cells. Dump^{neg} Tom⁺ thymocytes were uniformly $Gads$ -negative in all thymic compartments (Figure 1E), thus establishing Tom⁺ as a marker that reliably identifies $Gads^{iKO}$ thymocytes in our experimental system.

Thymocyte development begins in the DN quadrant, which is first populated by bone-marrow-derived common lymphoid progenitors [51]. While variable between mice, the frequency of Tom⁺ DN thymocytes strongly resembled the frequency of Tom⁺ PBLs in the same mouse (Figure 1F). This observation suggests that tamoxifen triggered UBC-Cre-ERT2-mediated recombination with comparable efficiency in thymic progenitor cells and in preexisting peripheral T-cell compartments.

As discussed in further detail below, the inherently chimeric nature of our experimental system allows us to highlight $Gads$ -dependent developmental transitions by performing in-mouse comparisons of Tom⁺ ($Gads^{iKO}$) and Tom⁻ ($Gads$ -expressing) thymocytes, developing side by side within the same thymic environment. To best reflect intra-thymic competition between $Gads$ -expressing and -ablated cells, we prefer to perform in-mouse comparisons in cohorts of Cre⁺ mice in which no more than 80% of DN thymocytes are Tom⁺. On the other hand, the chimeric nature of our model confounds the calculation of the absolute number of thymocytes per compartment, due to the presence of the opposite genotype that partially occupies each thymic niche. To bypass this difficulty, we restricted the calculation of absolute cell numbers to cohorts of Cre⁺ mice in which greater than 95% of DN thymocytes were Tom⁺.

As a representative illustration of the in-mouse comparison approach, we note that the frequency of Tom⁺ $Gads^{iKO}$ thymocytes was highest in the DN compartment (Figure 1E, bottom left). As DN thymocytes progressed to the DP and SP compartments, the frequency of Tom⁺ $Gads^{iKO}$ thymocytes markedly decreased (Figure 1E, upper panels and bottom right). This simple experiment therefore provides preliminary insight into the impaired developmental progression of $Gads^{iKO}$ DN thymocytes, relative to wild-type thymocytes within the same mouse.

2.4 | Cell-Autonomous Phenotypes of $Gads^{iKO}$ (Tom⁺) Thymocytes

Following tamoxifen treatment, the contemporaneous development of Tom⁺ ($Gads^{iKO}$) and Tom⁻ ($Gads$ -expressing) thymocytes within the same mouse provided an opportunity to assess the cell-autonomous effects of $Gads$ on thymocyte development. To implement this strategy, we chose cohorts of Cre⁺ mice in which 60–80% of DN thymocytes were Tom⁺. In practice, we chose the cohort based on the frequency of Tom⁺ PBLs observed in a test bleed, as this measure correlated quite strongly to the frequency of Tom⁺ DN thymocytes (Figure 1F). To focus on conventional T cell development, we used a dump gate to exclude non-T cell lineages, as well as NK1.1⁺ and TCR $\gamma\delta$ ⁺ thymocytes. We followed thymic progression within the dump^{neg} population while gating separately on $Gads$ -expressing (Tom⁻) and $Gads^{iKO}$ (Tom⁺) thymocytes (Figure 2A).

Tom⁺ ($Gads^{iKO}$) thymocytes exhibited a partial block at the DN to DP transition compared with Cre⁻ thymocytes (Figure 2A). This developmental block was reflected in a marked, statistically significant increase in the frequency of DN thymocytes (Figure 2B, left) and reduced frequency of CD4 SP thymocytes (Figure 2B, middle), whereas the frequency of CD8 thymocytes

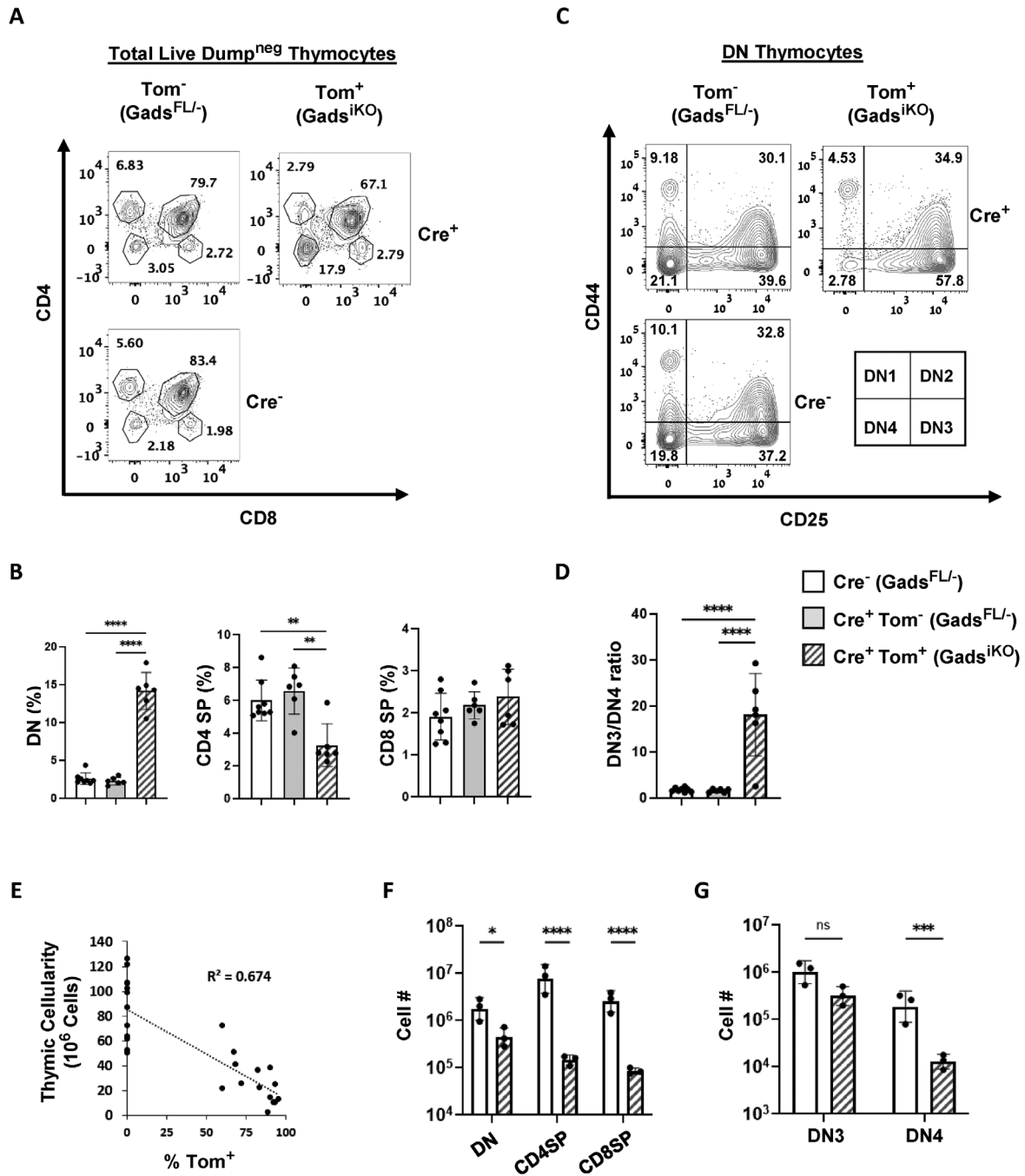


FIGURE 2 | Cell autonomous developmental phenotypes of Gads^{iKO} thymocytes. Mice were tamoxifen-treated as in Figure 1C, and thymi were collected 2–2.5 weeks after starting tamoxifen. We assessed developmental markers in live thymocytes while employing a mixture of FITC-labeled surface-staining antibodies (anti-mouse NK1.1, TCRγ/δ, TER-119, Gr-1, CD11b, and B220) to exclude NK1.1⁺ and TCRγδ⁺ thymocytes, as well as erythrocyte, granulocyte, macrophage, monocyte, and B cell lineages. (A–D) To facilitate within-mouse comparisons, we analyzed a cohort of Cre⁺ mice in which 60–80% of PBLs were Tom⁺. *n* = 8 Cre⁻ and 6 Cre⁺ mice. (A) Representative distribution of CD4 and CD8 surface markers within the live, dump^{neg} population, assessed while gating separately on Tom⁻ (Gads^{FL/-}) and Tom⁺ (Gads^{iKO}) thymocytes. (B) The frequency of thymocytes found within each of the indicated subpopulations, defined in (A). (C) Representative progression through DN substages was assessed while gating on live, dump^{neg} Tom⁺ and Tom⁻ DN (CD4⁺ CD8⁻) thymocytes. (D) The DN3 to DN4 ratio was calculated based on the gating strategy shown in C. (E) Reduced thymic cellularity in Gads^{iKO} mice. Total thymic cellularity is plotted as a function of the frequency of Tom⁺ PBLs. Cre⁻ mice are plotted on the Y-axis. A linear regression confirmed a tendency to reduced thymus size with increased frequency of Tom⁺ cells. To increase the number of data points, this panel combines data from multiple experiments in which the thymus was collected 1.5–2.5 weeks after starting tamoxifen. *n* = 13 Cre⁻ and 14 Cre⁺ mice. (F, G) To enable accurate accounting of total thymocytes per compartment, we analyzed a cohort of Cre⁺ mice in which greater than 95% of PBLs were Tom⁺. *n* = 3 mice of each genotype. (F) The absolute number of thymocytes within each of the indicated populations. (G) The absolute number of DN3 and DN4 thymocytes. The legend relates to all bar graphs: Cre⁻ (Gads^{FL/-}), open bars; Cre⁺Tom⁻ (Gads^{FL/-}), grey bars; Cre⁺Tom⁺ (Gads^{iKO}), striped bars. Error bars indicate the standard deviation. Statistical significance was determined by a one-way ANOVA, Tukey's multiple comparison test (B, D), or by a two-way ANOVA, Šidák's multiple comparisons test (F, G).

was unchanged (Figure 2B, right). Within the DN compartment, $Gads^{iKO}$ thymocytes exhibited a partial block at the DN3 to DN4 transition (Figure 2C), leading to a marked increase in the ratio of DN3 to DN4 cells (Figure 2D). In all of these traits, $Gads^{iKO}$ thymocytes closely resemble the germline $Gads^{KO}$ (compare Figure 2A–D with Figure S1B–G). In contrast, Cre^+Tom^- thymocytes, developing within the same thymic environment, phenocopied Cre^- thymocytes, and both were statistically different from $Gads^{iKO}$ thymocytes (Figure 2A–D).

We considered the possibility that selective impairment of $Gads^{iKO}$ thymocytes may allow for compensatory progression of Tom^- thymocytes, which would crowd out their Tom^+ counterparts. Since $Gads$ -deficient mice are characterized by a small thymus (Figure S1A and [46, 47]), we reasoned that cell-autonomous effects of $Gads$ would result in a small thymus whereas the compensatory progression of Tom^- thymocytes may maintain normal thymic cellularity. Thymic cellularity substantially decreased in tamoxifen-treated Cre^+ mice, relative to Cre^- littermates, and this trend was most apparent in mice with the highest frequency of Tom^+ PBLs (Figure 2E).

It is interesting to calculate the absolute number of cells within each thymic compartment. To avoid interference from the opposite genotype, we performed this calculation in a cohort of Cre^+ mice in which greater than 95% of DN thymocytes were Tom^+ . Despite the profound reduction in thymic cellularity (see Figure 2E), the number of DN cells was only moderately reduced (Figure 2F). Further consistent with a profound block in β -selection, the absolute number of DN3 cells was not significantly changed, but the DN4 cell number was reduced by more than 15-fold (Figure 2G). Further along the developmental pathway, CD4 and CD8 SP thymocytes decreased by approximately 60- and 30-fold, respectively (Figure 2F). These results mirror the published characterizations of a germline $Gads$ -deficient mouse model [45, 47], and provide confidence that our inducible deletion model faithfully recapitulates the phenotypes associated with deletion of $Gads$.

Taken together, our results suggest that the phenotypic effects of deleting $Gads$ are predominantly cell-autonomous, with Tom^- thymocytes largely following normal developmental pathways, while Tom^+ ($Gads^{iKO}$) thymocytes within the same mouse phenocopy germline $Gads$ -deficient thymocytes.

2.5 | Three Metrics for the Identification of $Gads$ -Dependent Developmental Junctions

2.5.1 | Competitive Developmental Progression of Tom^+ Cells

The chimeric nature of $Gads^{iKO}$ mice suggested a simple strategy to identify developmental junctions at which $Gads$ exerts its effects. We posited that the frequency of Tom^+ thymocytes should decrease as cells pass through $Gads$ -dependent developmental junctions. Conversely, the frequency of Tom^+ thymocytes may remain the same or even increase in $Gads$ -independent lineages.

Consistent with the established impairment of $Gads$ -deficient thymocytes at the β -selection checkpoint [46, 47], the frequency of

Tom^+ cells dropped substantially as thymocytes passed into DN4 (Figure 3A). To facilitate statistical comparisons between mice, we normalized the frequency of Tom^+ cells in each compartment to their frequency in the DN1 compartment of the same mouse. The marked drop in the normalized frequency of Tom^+ ($Gads^{iKO}$) thymocytes at the transition from DN3 to DN4 confirmed a profound impairment of β -selection (Figure 3B).

Following progression to the DP compartment, $\alpha\beta$ -TCR-mediated recognition of self-peptide-MHC antigens may induce positive selection and consequent passage to the SP compartments. We discerned a drop in the relative frequency of Tom^+ cells at the DP to CD4 SP boundary, suggesting a mild impairment of positive selection; however, it did not reach statistical significance in this analysis (Figure 3B). This discrepancy raised questions about the mode of developmental progression. Are $Gads^{iKO}$ cells fully capable of undergoing positive selection? Or might they progress through the developmental compartments as unselected cells?

2.5.2 | Developmentally-Associated Upregulation of CD69 and TCR β

To better address the role of $Gads$ in positive selection, we turned to additional markers. In a previously described approach [12], five sequential stages of thymic development are distinguished by the abundance of surface TCR and CD69, as outlined in Figure 3C, bottom right. Thymocytes begin their development as TCR $^-$ CD69 $^-$ cells (population 1), with TCR β expression increasing moderately following the generation of a mature $\alpha\beta$ -TCR $^+$ (population 2). Positive selection triggers transient expression of CD69 (populations 3 and 4), along with a marked increase in surface TCR (population 4). TCR expression subsequently remains high, whereas CD69 decreases upon maturation of SP thymocytes (population 5).

Upon ablation of $Gads$, the frequency of population 1 thymocytes markedly increased, whereas populations 2 and 4 decreased (Figure 3C,D). These changes appeared to be cell-autonomous, as Tom^- thymocytes from the same Cre^+ mice closely resembled $Gads$ -expressing thymocytes from Cre^- mice (Figure 3C).

To assess how $Gads$ affects the absolute number of thymocytes per group, we compared a cohort of Cre^- mice to a cohort of Cre^+ mice in which greater than 95% of DN thymocytes were Tom^+ . Given the low thymic cellularity of the Cre^+ mice (see Figure 2E), we observed statistically significant decreases in the cellularity of all five populations (Figure 3E). This type of analysis is therefore not a useful way to distinguish $Gads$ -dependent junctions.

To more robustly identify $Gads$ -dependent junctions, we performed in-mouse comparisons to determine the relative advancement of Tom^+ ($Gads^{iKO}$) and Tom^- ($Gads$ -expressing) thymocytes through each of the five stages (Figure 3F). This analysis is not affected by thymic cellularity, as cells of both genotypes compete within the same thymic environment. To facilitate statistical analysis, we normalized the frequency of Tom^+ cells in each population to their frequency in population 1 of the same mouse. The relative frequency of Tom^+ thymocytes decreased significantly at two junctions, first between populations 1 and 2,

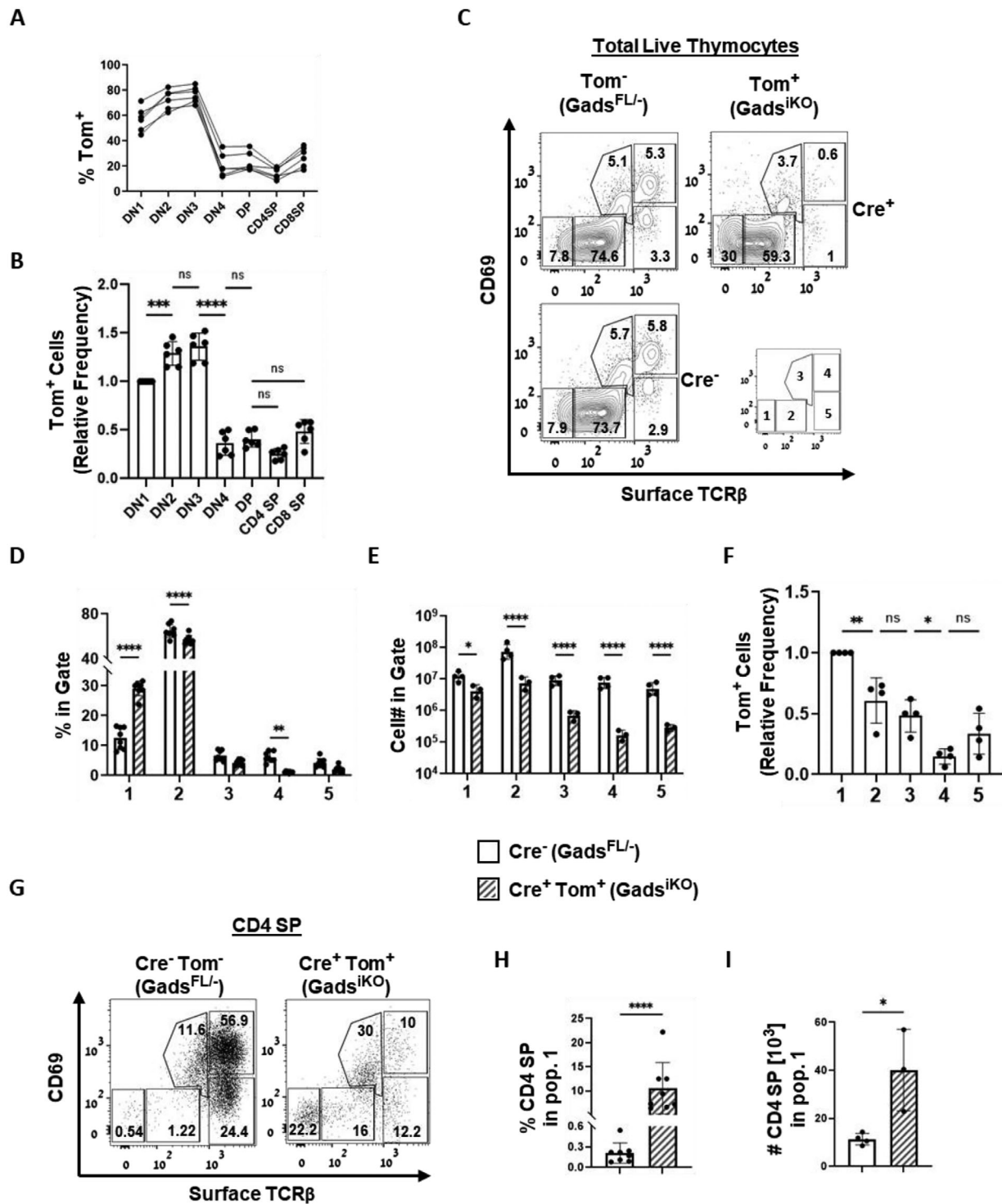


FIGURE 3 | Identification of Gads-dependent developmental junctions. (A, B) The frequency of Tom⁺ thymocytes was determined within each of the indicated populations. These data derive from the mouse cohort and gating strategy depicted in Figure 2A–D (A) Raw frequencies observed in 6 Cre⁺ mice. (B) To facilitate statistically valid comparisons between mice, the frequency of Tom⁺ cells in each population was normalized to their frequency in the DN1 compartment of the same mouse. (C–I) 2.5–3.5 weeks after starting tamoxifen treatment, surface expression of CD69 and TCRβ was assessed in the indicated populations. $n = 8$ mice of each genotype, of which 4 Cre⁻ and 3 Cre⁺ mice (with %Tom⁺ DN thymocytes >95%) were used for calculating total cell numbers. (C) Representative result, obtained while gating on total live thymocytes. (D, E) The frequency (D) and absolute number (E) of cells within each of the populations defined in (C). (F) The relative frequency of Tom⁺ thymocytes within each of the populations shown in (C). To facilitate within-mouse comparisons, this analysis included Cre⁺ mice in which 70–90% of DN thymocytes were Tom⁺. The frequency of Tom⁺ cells in each gate was normalized to their frequency in population 1 of the same mouse. $n = 4$ Cre⁺ mice. (G) Representative result, obtained while gating on CD4 SP thymocytes, as defined in Figure 2A. (H–I) The frequency (H) and absolute number (I) of population 1 cells among the indicated CD4 SP thymocytes. The legend relates to panels (D), (E), (H), (I): Cre⁻ (Gads^{FL/-}), open bars; Cre⁺Tom⁺ (Gads^{iKO}), striped bars. Statistical significance was determined by an ANOVA, Šidák's multiple comparisons test, either one-way (panels B and F), two-way (panels D–E), or by unpaired *t*-test (panels H–I).

and then again between populations 3 and 4 (Figure 3F). This analysis provides strong evidence that Gads^{iKO} thymocytes exhibit two distinct developmental defects: impaired β -selection at the population 1 to 2 boundary, and impaired positive selection at the population 3 to 4 boundary.

As a representation of the earliest stages of thymic development, population 1 (TCR β ⁻ CD69⁻) cells are usually restricted to the DN and DP quadrants [12]. We were therefore surprised to observe a high prevalence of population 1 cells within the Gads^{iKO} CD4 SP compartment (Figure 3G). Both the frequency and the number of Gads^{iKO} population 1 CD4 SP cells far outnumbered their prevalence among Cre⁻ CD4 SP thymocytes (Figure 3H,I).

Taken together, this analysis suggests that in Gads-deficient mice, reduced positive selection, reflected in the reduced frequency of group 4 Tom⁺ thymocytes (Figure 3C–F), is accompanied by the aberrant progression of group 1, unselected Tom⁺ thymocytes as far as the CD4 SP compartment (Figure 3G–I).

2.5.3 | Developmentally-Associated Upregulation of CD5 and TCR β

To further illuminate the developmental progression of Gads^{iKO} thymocytes, we assessed the expression of CD5 in conjunction with surface TCR β . CD5 is a valuable marker of TCR responsiveness that can be used to assess multiple developmental transitions, as it is first expressed at β -selection, and further increases upon positive selection [8]. Whereas CD69 is transiently expressed [12], high expression of CD5 stably marks positively selected thymocytes. Most importantly, considerable evidence suggests that the cell surface abundance of CD5 reflects the intensity of intrathymic responsiveness to self-peptide-MHC [4, 8].

In a previous study, overexpression of a dominant negative allele of Gads moderately reduced the expression of CD5 within the DN compartment [52]; however, this marker was not followed through subsequent developmental stages. Moreover, to the best of our knowledge, CD5 expression patterns were never described in Gads-deficient mice. Thus, the role of Gads in mediating CD5 expression is largely unknown.

To focus on conventional T cell development, in Figures 4A–K we measured the surface expression of TCR β , CD5, and other markers, while employing a strict dump gate to exclude TCR $\gamma\delta$ ⁺ and NK1.1⁺ thymocytes as well as multiple non-T cell lineages. In this experiment, we also used an isotype control to discern the boundary between TCR β ⁻ and TCR β ^{lo} (data not shown). Consistent with an early block in thymic development, Gads^{iKO} thymocytes were profoundly skewed toward a CD5⁻TCR β ⁻ phenotype and exhibited a steep drop in the frequency of CD5^{hi}TCR β ^{hi} thymocytes (Figure 4A,B). The absolute number of Gads^{iKO} CD5⁻TCR β ⁻ thymocytes did not significantly increase, but the absolute number of Gads^{iKO} CD5^{hi}TCR β ^{hi} thymocytes decreased by more than 50-fold (Figure 4C).

Consistent with the expression of CD5 upon β -selection and its further increase upon recognition of self-peptide-MHC, most

Gads-expressing DP cells were CD5⁺. CD5 expression was markedly lower in Gads^{iKO} DP thymocytes (Figure 4D) and both the frequency and number of CD5⁻TCR β ⁻ cells were markedly increased (Figure 4E,F). Curiously, CD5⁻TCR β ⁻ Gads^{iKO} DP thymocytes exhibited a CD44^{lo}CD25⁺ phenotype (Figure 4G), which is reminiscent of DN thymocytes undergoing β -selection. This observation supports the possibility that Gads^{iKO} thymocytes may experience an uncoupling of developmental progression from the completion of β -selection, resulting in aberrant progression of thymocytes from DN to DP, in the absence of β -selection.

The aberrant progression of CD5⁻TCR β ⁻ Gads^{iKO} thymocytes continued into the CD4 SP compartment. Whereas wild-type CD4 SP thymocytes were overwhelmingly CD5^{hi} and TCR β ^{hi}, the Gads^{iKO} CD4 SP compartment also included a prominent CD5⁻TCR β ⁻ subpopulation (Figure 4H). Indeed, both the frequency and the number of Gads^{iKO} CD5⁻TCR β ⁻ CD4 SP cells far outnumbered their prevalence among Cre⁻ CD4 SP thymocytes (Figure 4I,J). As in the DP compartment, the vast majority of Gads^{iKO} CD5⁻TCR β ⁻ CD4 SP thymocytes exhibited a CD44^{lo}CD25⁺ phenotype (Figure 4K), again reminiscent of DN thymocytes undergoing β -selection, and providing further evidence that Gads^{iKO} thymocytes may experience an uncoupling of developmental progression from the completion of both β - and positive-selection.

Despite its atypical phenotype, the CD5⁻ CD4 SP population was clearly part of the T cell lineage, as demonstrated by its strong intracellular staining with TCR β (Figure 4L), and by its exclusion from the strict dump gate that was used in Figures 4A–K.

A similar CD5⁻ TCR β ^{neg-lo}CD4 SP population was found in germline Gads-deficient mice (Figure 4M). Both the prevalence and the absolute number of CD5⁻TCR β ^{neg-lo} CD4 SP thymocytes were markedly increased in germline Gads-deficient mice as compared with age-matched wild-type mice (Figure 4N,O). This result suggests that an atypical CD5⁻TCR β ^{neg-lo} population that progresses as far as the CD4 SP compartment is a conserved feature of Gads-deficient thymocyte development. An additional, aberrant population of CD5^{hi}TCR β ^{neg-lo} CD4 SP thymocytes was reproducibly observed in germline Gads-deficient mice (Figure 4M) but was not further characterized.

Taken together, our results identify three developmental processes that are impaired in the absence of Gads: [1] β -selection, [2] positive selection, and [3] the obligatory coupling of developmental progression to the above events. These results encouraged us to closely examine the developmental state of Gads^{iKO} thymocytes within each compartment while using CD5 as a marker for signaling competence.

2.6 | Divergent β - and $\gamma\delta$ -TCR Signaling Competence in Gads^{iKO} DN Thymocytes

The developmental progression of DN thymocytes is driven by signaling events that are initiated either by the pre-TCR, triggering β -selection, or by the $\gamma\delta$ TCR. CD5 expression within the DN compartment is markedly reduced upon TCR signaling pathway impairment [8], thus establishing CD5 as a useful marker

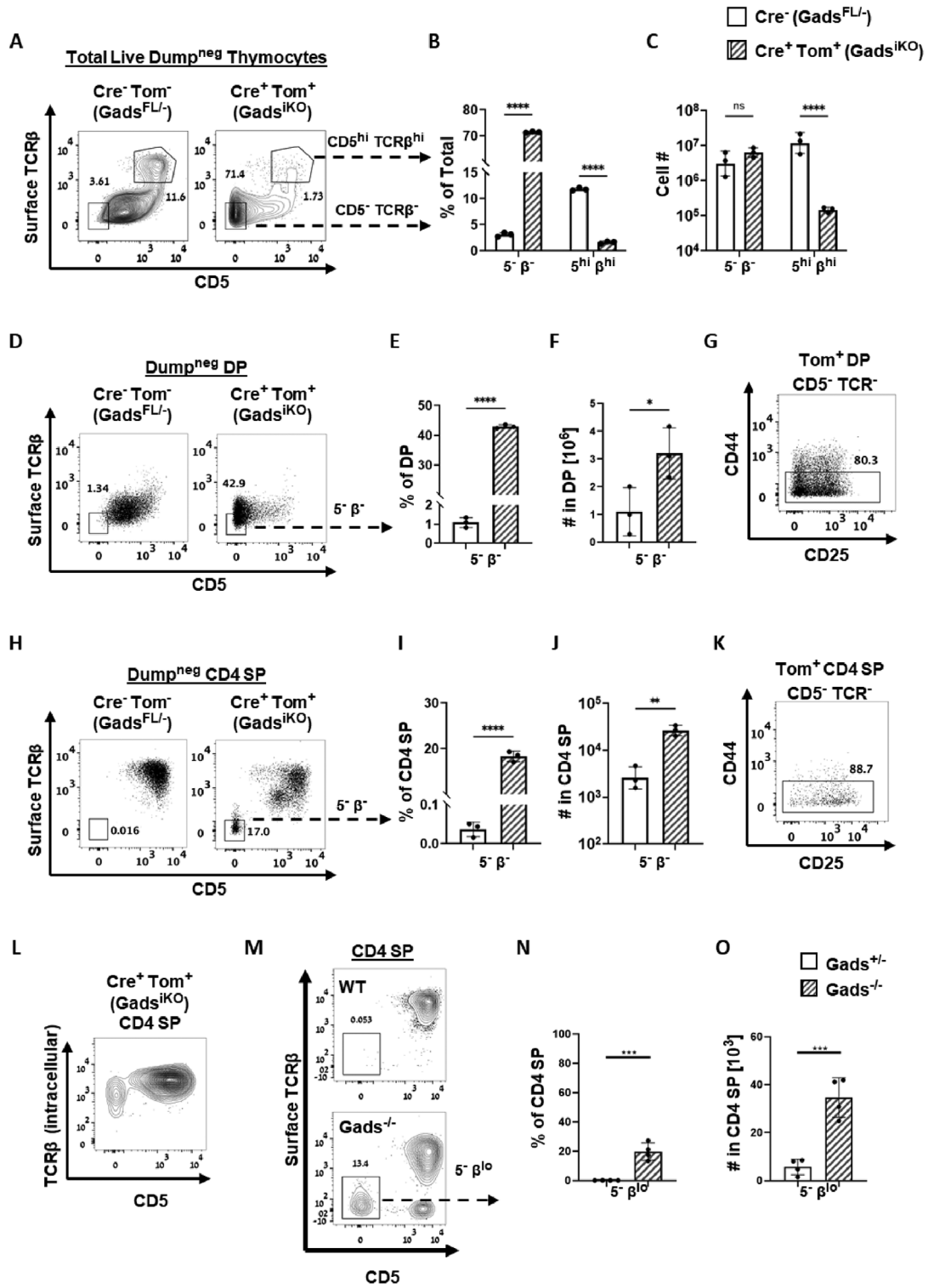


FIGURE 4 | Developmental progression of TCR-inexperienced $Gads^{iKO}$ thymocytes. (A–K) 2.5 weeks after starting tamoxifen treatment, we assessed surface markers, while employing a strict dump gate (anti-mouse NK1.1, TCR γ/δ , TER-119, Gr-1, CD11b, CD11c, B220, CD19, and Fc ϵ RI α) to exclude NK1.1⁺ and TCR $\gamma\delta$ ⁺ thymocytes, as well as non-T cell lineages. $n = 3$ mice of each genotype; comprising a cohort of Cre⁺ mice in which >95% of DN thymocytes were Tom⁺. Results are presented while gating on total live (A–C), DP (D–G), or CD4 SP thymocytes (H–K). (A, D, H) Representative expression of CD5 and TCR β . Gates indicate populations of interest: CD5^{hi}TCR β ^{hi} and/or CD5^{hi}TCR β ^{lo}. (B, C, E, F, I, J) The frequency (B, E, I) and absolute number (C, F, J) of thymocytes found within each population of interest, as indicated on the x-axis. (G, K) Expression of CD44 and CD25 within the CD5^{hi}TCR β ^{lo} $Gads^{iKO}$ DP (G) and CD4 SP (K) populations. (L) 2.5 weeks after starting tamoxifen treatment, we assessed the expression of intracellular TCR β and CD5 in $Gads^{iKO}$ CD4 SP thymocytes. (M–O) Surface expression of CD5 and TCR β in CD4 SP thymocytes from 8.5- to 9-week-old WT and germline $Gads$ KO mice. (M) Representative result. (N, O) The frequency (N) and absolute number (O) of CD5^{hi}TCR β ^{lo} cells, as defined in M. $n = 4$ mice of each genotype. The legend relates to all bar graphs: Cre⁻ ($Gads^{FL/-}$), open bars; Cre⁺Tom⁺ ($Gads^{iKO}$), striped bars. Statistical significance was determined by a two-way ANOVA, Šidák's multiple comparisons test (panels B and C), or unpaired t-test (panels E, F, I, J, N, O).

of pre-TCR signaling in situ. Here we used the CD5 and CD25 markers to explore how Gads affects TCR responsiveness and TCR-driven developmental progression in the context of β - and δ -selection.

To identify DN thymocytes that may be experiencing TCR signaling, we gated on the CD44^{lo} DN population, which encompasses both DN3 and DN4 (DN3+4 gate, Figure 5A, top), while using intracellular staining to distinguish cells that had rearranged either the β or $\gamma\delta$ chains of the TCR (Figure 5A, bottom). This experiment was conducted while using a dump gate to exclude non-T cell lineages and NK1.1⁺ DN thymocytes. Among Gads^{iKO} DN3+4 thymocytes, the frequency of TCR β ⁺ cells decreased, whereas the frequency of TCR^{neg} cells increased and the frequency of TCR $\gamma\delta$ ⁺ cells did not significantly change (Figure 5B).

To obtain additional insight, we used the CD5 and CD25 markers to discern TCR responsiveness and developmental progression within each subpopulation. As expected, the TCR^{neg} (TCR β ⁻ TCR $\gamma\delta$ ⁻) DN3+4 population, which is necessarily TCR-inexperienced, was overwhelmingly CD25^{hi} and CD5⁻, both in the presence and in the absence of Gads (Figure 5C, top panels). This result establishes the baseline to which TCR-expressing DN thymocytes should be compared.

Consistent with ongoing β -selection, Gads-expressing, TCR β ⁺ DN3+4 thymocytes were found on a trajectory of increased CD5 and decreased CD25. We defined two gates of interest along this trajectory. The post- β -selection gate (Figure 5C, middle panels) encompasses TCR β ⁺ cells that have responded to pre-TCR signaling, as evidenced by their expression of CD5, and transited into DN4, as evidenced by their loss of CD25. The incomplete β -selection gate encompasses TCR β ⁺ cells that reduced CD25 to a variable extent, without upregulating CD5 (Figure 5C, middle panels). In the absence of Gads, the frequency of incomplete β -selection increased dramatically, with a corresponding decrease in the frequency of post- β -selection DN3+4 thymocytes (Figure 5D, left). A different developmental pattern was observed among TCR $\gamma\delta$ -expressing DN3+4 thymocytes. The vast majority of these cells attained the post- δ -selection, CD25⁻CD5⁺ state, irrespective of Gads expression (Figure 5C, bottom panels).

To determine the effect of Gads on the absolute number of post- β - or δ -selection DN cells per thymus, we analyzed a cohort of Cre⁺ mice in which greater than 95% of DN thymocytes were Tom⁺. The absolute number of post- β -selection DN3+4 cells per thymus was profoundly reduced upon ablation of Gads (Figure 5D, right). In contrast, neither the frequency nor the number of post- δ -selection (CD25⁻CD5⁺) $\gamma\delta$ DN3+4 cells was significantly altered by ablation of Gads (Figure 5E). Our results are consistent with the findings of Zeng et al., who noted a profound impairment in the transition of germline Gads-deficient TCR β -expressing thymocytes from DN3 to DN4, whereas Gads-deficient TCR $\gamma\delta$ -expressing DN thymocytes were less affected [45]. Further extending this paradigm, our examination of CD5 expression suggests that pre-TCR signaling strongly depends on Gads whereas TCR $\gamma\delta$ signaling appears to be relatively Gads-independent.

2.7 | TCR-Induced Progression Through the DP Compartment Depends on Gads

Despite prominent impairment of β -selection, Gads-deficient thymocytes populate the DP compartment (see Figure 2A and Figure S1B). Several investigators have estimated TCR-driven progression through the DP compartment by subdividing it according to the surface expression of CD5 and TCR β [11, 53]. In a similar fashion, we subdivided the DP compartment into nonresponding (CD5⁻), low-responding (CD5^{med}TCR β ^{med}), and high-responding cells (CD5^{hi}TCR β ^{hi}) (Figure 6A). When detected by intracellular staining, TCR expression was comparable in Gads^{iKO} and Gads-expressing DP thymocytes (Figure 6B). Nevertheless, Gads^{iKO} (Tom⁺) DP thymocytes were significantly more likely to be nonresponding and less likely to be low or high-responding (Figure 6C). The DP subset distribution was similarly skewed in germline Gads-deficient mice (Figure 6D), suggesting that a predominantly CD5⁻ (nonresponding) DP phenotype is a previously unreported, core characteristic of Gads-deficient thymocytes.

The predominantly nonresponding phenotype of Gads^{iKO} DP thymocytes provides evidence for a TCR signaling defect. Nevertheless, a small population of Gads^{iKO} DP thymocytes expressed CD5 (Figure 6A), raising the possibility that a subset of Gads^{iKO} DP thymocytes may be TCR signaling-competent. To test this notion, we measured TCR-induced calcium flux, using an ex vivo, flow cytometry-based assay, while gating on CD5⁺ (presumptively signaling competent) DP thymocytes, as defined in Figure 6E. Intracellular staining verified that Tom⁺ DP cells within the CD5⁺ gate were indeed Gads-deficient (Figure 6F, right), moreover, surface TCR β expression was well matched between CD5⁺ Tom⁺ and CD5⁺ Tom⁻ cells (Figure 6F, left). To measure calcium, a mixture of Tom⁺ and Tom⁻ thymocytes was fluorescently labeled with anti-CD4, anti-CD8, and anti-CD5, along with biotinylated stimulatory antibodies. As a control for cell viability and intact calcium stores, ionomycin-induced calcium flux was not affected by Gads (Figure 6G, bottom panels).

After measuring baseline calcium at 37°C, cells were triggered by streptavidin-mediated co-cross-linking of CD3, CD4, and CD8, to mimic co-receptor-dependent recognition of MHC. Intracellular calcium increased in Gads-expressing (Tom⁻) CD5⁺ DP thymocytes, but this response was blunted in Gads^{iKO} CD5⁺ DP thymocytes (Figure 6G, top panels). When analyzed on a single-cell basis, the frequency of responding CD5⁺ DP thymocytes was reduced 6.8-fold in the absence of Gads (Figure 6H). These data confirm a profound TCR signaling defect in Gads-deficient DP thymocytes, even within the CD5⁺, potentially responsive gate.

2.8 | Gads Facilitates Death by Neglect Within the TCR-Nonresponding DP Population

The $\alpha\beta$ -TCR repertoire is profoundly shaped by clonal cell death. Whereas strong recognition of self-peptide-MHC antigen triggers negative selection, peptide-MHC nonresponsive DP thymocytes are candidates for death by neglect [15]. In both cases, cells die by apoptosis; but whereas negative selection is more likely to occur in highly responsive (CD5^{hi}) cells, death by neglect occurs in low-responding (CD5^{neg-lo}) cells [11].

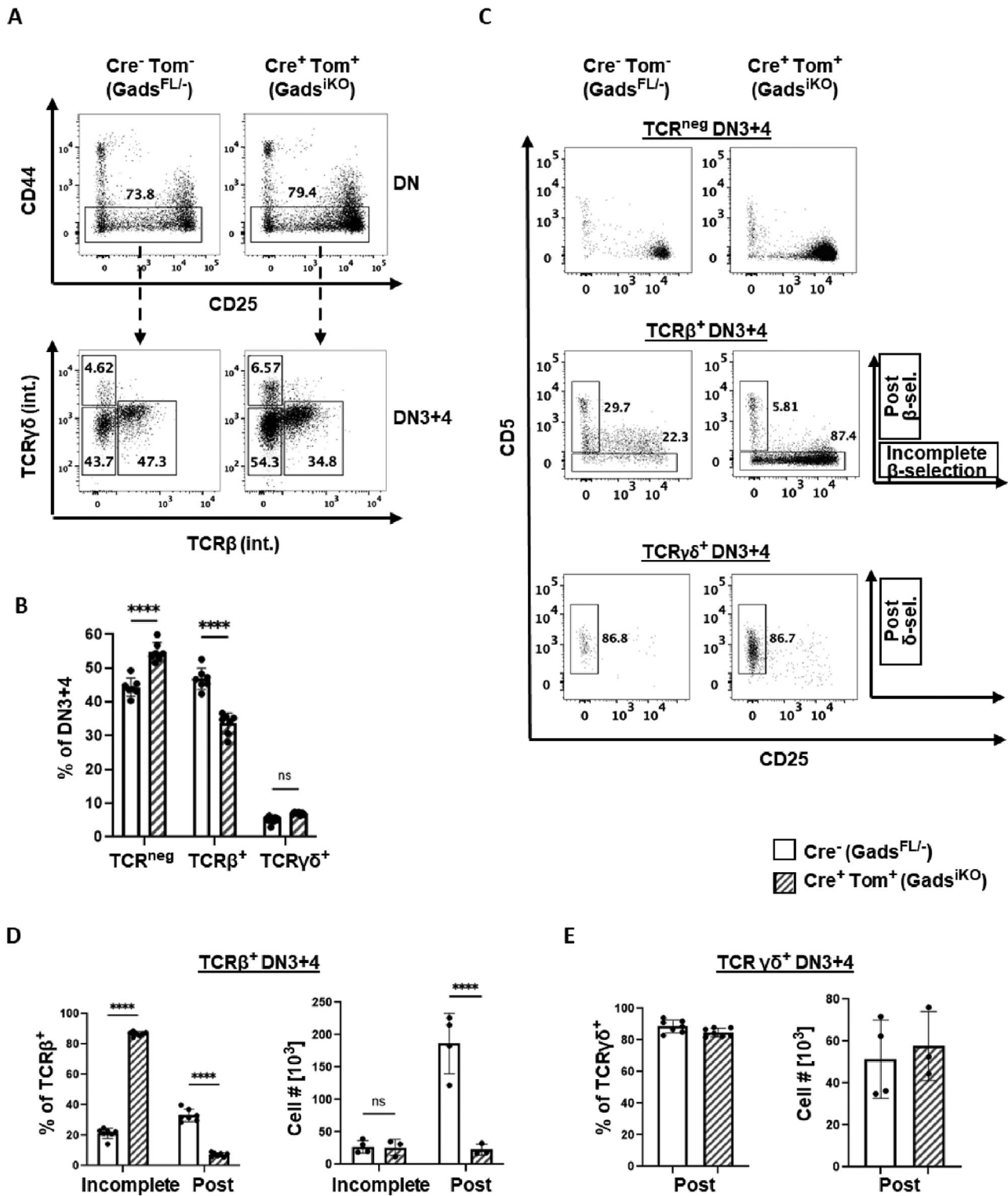


FIGURE 5 | Divergent β - and $\gamma\delta$ -TCR signaling competence in Gads^{iKO} DN thymocytes. Developmental surface markers were assessed in live DN thymocytes while staining intracellularly for TCR- β and - $\gamma\delta$, and employing a dump gate (anti-mouse NK1.1, CD8 α , TER-119, Gr-1, CD11b, and B220) to exclude CD8⁺ and NK1.1⁺ thymocytes, and non-T cell lineages. (A) The gating strategy used to determine the expression of TCR- β and - $\gamma\delta$ within the CD44^{lo} (DN3+4) gate. (B) Frequency of TCR expression within the DN3+4 gate. (C) Representative expression of CD5 and CD25 within each DN3+4 TCR expression gate, as defined in A. The gates defined at right were used to differentiate the early and late stages of β - and δ -selection. (D) The frequency (left) and absolute number (right) of incomplete and post- β -selection cells within the TCR β ⁺ DN3+4 gate. (E) The frequency (left) and absolute number (right) of post- δ -selection cells within the TCR $\gamma\delta$ ⁺ DN3+4 gate. $n = 7$ mice of each genotype, with thymi harvested 2.5 weeks after starting tamoxifen treatment. Where relevant, the absolute number of cells per thymus was determined using a subset of 4 Cre⁻ mice and 3 Cre⁺ mice in which the frequency of Tom⁺ DN thymocytes was greater than 95%. The legend relates to all bar graphs: Cre⁻ (Gads^{FL/-}), open bars; Cre⁺ Tom⁺ (Gads^{iKO}), striped bars. Statistical significance was determined by a two-way ANOVA, Šidák's multiple comparisons test (panels B and D), or unpaired t -test (panel E).

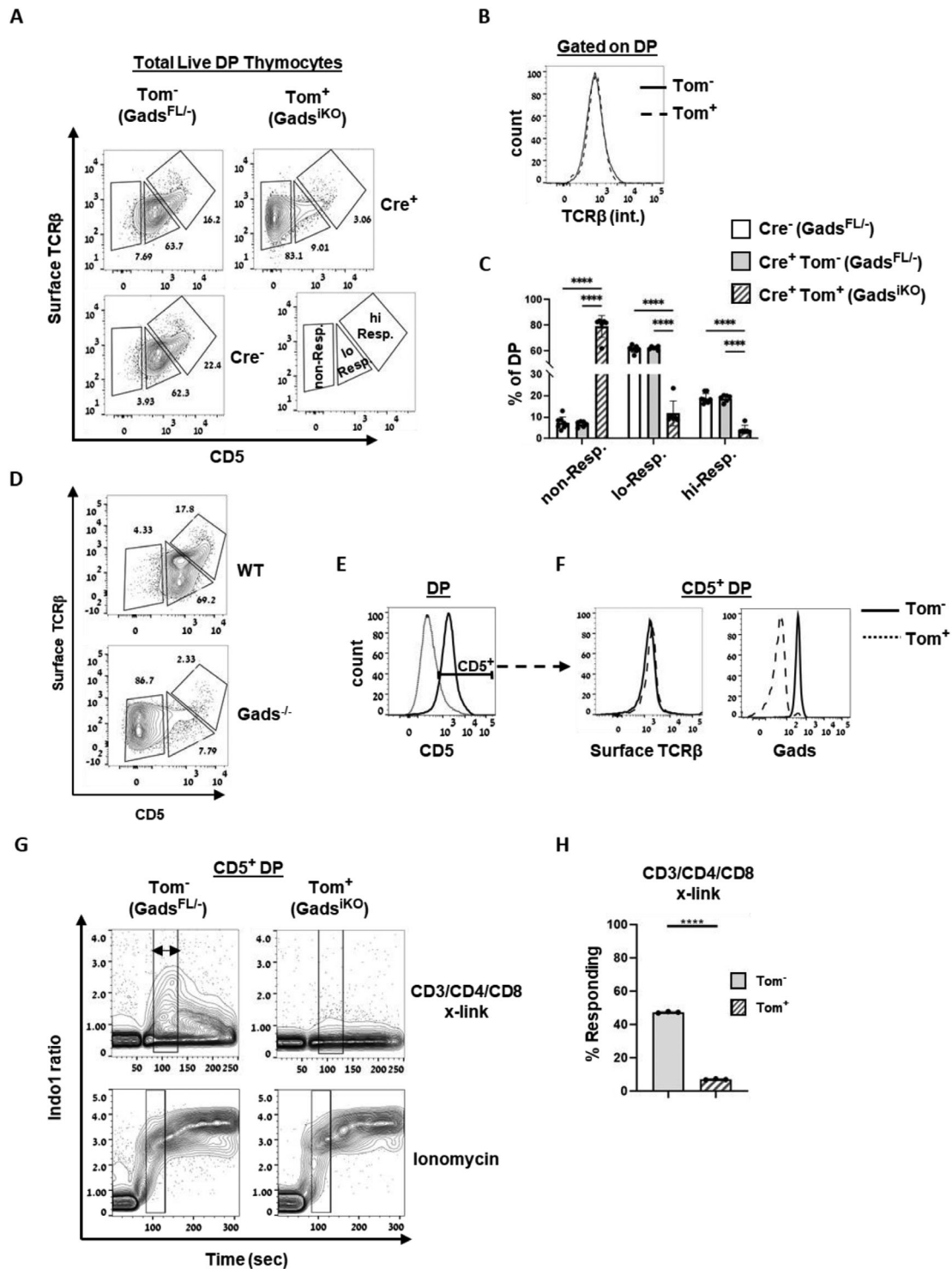


FIGURE 6 | TCR-induced progression through the DP compartment depends on Gads. (A–C) 2–2.5 weeks after starting tamoxifen treatment, we assessed surface TCRβ and CD5 expression in live DP thymocytes. (A) Representative result. DP populations of interest are defined at the bottom right. (B) TCRβ expression within the DP compartment was detected by intracellular staining. (C) The frequency of DP cells within each of the populations of interest defined in (A). Statistical significance was determined by a two-way ANOVA, Šidák's multiple comparisons test. (D) Representative surface TCRβ and CD5 expression in DP thymocytes from 8.5- to 9-week-old WT and germline Gads KO mice. (E–H) TCR responsiveness within the CD5⁺ DP gate. Two weeks after starting tamoxifen treatment, Tom⁺ and Tom⁻ thymocytes were mixed together and stained with the calcium indicator, indo1, fluorescent cell surface markers, and biotinylated stimulatory antibodies (CD3, CD4, and CD8). (E) Gating strategy, calcium was measured while gating on this CD5⁺ DP gate. (F) Expression of surface TCR and intracellular Gads within the CD5⁺ gate, as defined in E. (G) Representative calcium fluorimetry result. The experiment was performed by flow cytometry at 37°C, with stimulation initiated at the 60 s time point by the addition of streptavidin (top panels) or ionomycin (bottom panels). The indo1 ratio is shown as a function of time while gating on CD5⁺, Tom⁺, or Tom⁻, DP thymocytes. The double-headed arrow marks a ~50 s time window within which we calculated the frequency of responding cells. (H) The frequency of cells exhibiting an indo1 ratio > 1 within the time window shown in (G). *n* = 3 repeats. Error bars were too small to depict. Statistical significance was determined by an unpaired *t*-test.

The marked accumulation of CD5⁺ Gads^{iKO} DP thymocytes raised the question of whether Gads may influence the process of death by neglect. To test this notion, we identified early apoptotic DP cells by measuring annexin V staining, while gating on four distinct live (Zombie^{neg}) DP populations, distinguished by their expression of CD5 (Figure 7A). Among these, the CD5^{lo} gate encompasses a population of low-responding cells that is common to Tom⁺ and Tom⁻ DP cells (Figure 7A). Within the CD5^{lo} live DP gate, Gads^{iKO} thymocytes exhibited a markedly lower frequency of annexin V positivity compared with Gads-expressing cells, whether from the same Cre⁺ mouse or a Cre⁻ mouse (Figure 7B).

Since death-inducing signals may derive from the thymic environment, we conducted a within-mouse, paired comparison of the rates of early apoptosis in Gads^{iKO} (Tom⁺) and Gads-expressing (Tom⁻) live DP thymocytes. The frequency of early apoptotic cells was markedly reduced in Gads^{iKO} CD5^{neg} and CD5^{lo} live DP thymocytes, compared with Tom⁻ thymocytes from the same gate and mouse (Figure 7C, two left panels). The reduction in apoptosis was much less prominent among Gads^{iKO} CD5^{hi} thymocytes, and no significant reduction was observed in Gads^{iKO} CD5^{med} DP thymocytes (Figure 7C, two right panels).

The mild reduction in early apoptosis among CD5^{hi} DP thymocytes is consistent with a previous study in which Gads was required for negative selection on a TCR transgenic background [46]. This impairment likely reflects the TCR signaling defect of Gads-deficient cells (see Figure 6G,H). Nevertheless, negative selection is difficult to assess on a polyclonal TCR background, due to potential skewing of the TCR repertoire among positively selected Gads^{iKO} thymocytes.

The reduction in early apoptosis among CD5^{neg-lo} cells was more pronounced and surprising, as these cells are TCR inexperienced. Indeed, it is not clear why the death of TCR-inexperienced cells should depend on TCR signaling machinery. One possible explanation is that many Gads^{iKO} thymocytes appear to pass into the DP compartment prior to completing β -selection (see Figure 4G). We therefore consider the possibility that completion of β -selection may be a prerequisite for susceptibility to death by neglect.

To more directly explore the susceptibility of Gads^{iKO} DP thymocytes to death by neglect, we modeled this process by culturing thymocytes in the absence of input from thymic stroma, as previously described [54]. Given the difficulty of accurately distinguishing tomato expression in dead cells, we chose to quantify DP cells that remained alive after one or two days in culture. To this end, we cultured Cre⁻ and Cre⁺ thymocytes separately, in the presence of reference microbeads, which we used to normalize the live cell count at each time point. The gating strategy used to identify live, DP, Cre⁻Tom⁻ or Cre⁺Tom⁺ thymocytes is depicted in Figure S2A. To calculate survival, we normalized the number of live DP cells at each time point to the number that were present at time zero. Gads^{iKO} DP thymocytes were fully capable of death in this experimental model; indeed, the survival of Gads^{iKO} DP cells was significantly lower than the survival of Cre⁻ (Gads-expressing) cells (Figure 7D). Taken together, these experiments suggest that despite an intrinsic capability to undergo death by neglect ex vivo (Figure 7D); Gads^{iKO} DP thymocytes exhibit a

lower rate of death by neglect within the thymic environment (Figure 7C, left two panels).

The intrathymic trigger of death by neglect is multifactorial and not yet well understood. Although TCR-mediated recognition of self-MHC can rescue DP thymocytes from death, Grebe et al. [55] suggested that death by neglect may be triggered upon ligation of CD8 by class I MHC, in the absence of TCR ligation. Consistent with this hypothesis, Grebe et al. developed an experimental system in which the death of preselection (CD5^{lo}) DP thymocytes can be induced by cross-linking CD8 [55].

To validate this model in our hands, we incubated wild-type thymocytes at 37°C with avidin beads that were either uncoated or coated with CD8- or CD4-biotin antibodies. Annexin V and DAPI staining were then assessed while gating on bead-bound DP cells, as defined in Figure S2B. We posited that bead-bound cells would be the best candidates for ligation-induced apoptosis. Within the bead-bound DP population, we gated on a CD5^{lo} gate that is common to Tom⁺ and Tom⁻ DP cells (Figure 7E) and corresponds to cells that are susceptible to death by neglect. We chose a 1 h time point to maximize the detection of early apoptotic cells (DAPI⁻ Annexin V⁺), while minimizing dead cells (DAPI⁺ Annexin V⁺). Under these conditions, CD8-biotin beads induced a marked increase in the frequency of early apoptotic cells, but no such increase was observed when thymocytes were incubated with CD4-biotin beads (Figure 7F).

To further explore potential reasons for the in vivo accumulation of nonresponding Gads^{iKO} DP thymocytes, we explored their relative susceptibility to CD8-induced death. To this end, we incubated a mixture of Tom⁺ and Tom⁻ thymocytes with uncoated or CD8-biotin-coated beads and analyzed the results while gating on the CD5^{lo} bead-bound DP population. Consistent with their lower rate of death by neglect in vivo (Figure 7B,C), Gads^{iKO} (Tom⁺) CD5^{lo} DP thymocytes exhibited a lower frequency of early apoptotic cells following their incubation with control, uncoated beads (Figure 7G, lower panels). CD8 crosslinking induced a marked increase in the frequency of early apoptotic cells (Figure 7G, upper panels); however, fewer apoptotic cells were observed in the absence of Gads.

Next, we repeated the experiment using beads coated with increasing amounts of anti-CD8 and calculated the induced death index. This measure depicts the net CD8-induced increase in the early apoptotic population, expressed as a fraction of the population that was live at baseline. The induced death index increased with increasing CD8 cross-linking; however, this index was substantially and significantly decreased in Gads^{iKO} thymocytes at all levels of stimulation, suggesting that Gads plays an important role in this model of CD8-induced death by neglect (Figure 7H).

Taken together, our data suggest two ways by which Gads regulates progression through the DP compartment. First, Gads is required for optimal responsiveness of DP thymocytes to self-peptide-MHC. This requirement is evidenced by the failure of Gads^{iKO} DP thymocytes to upregulate CD5 in vivo (Figures 6A–D), and by their markedly reduced TCR responsiveness ex vivo (Figure 6G,H). This interpretation is further reinforced by the reduced upregulation of CD69 in the absence of Gads

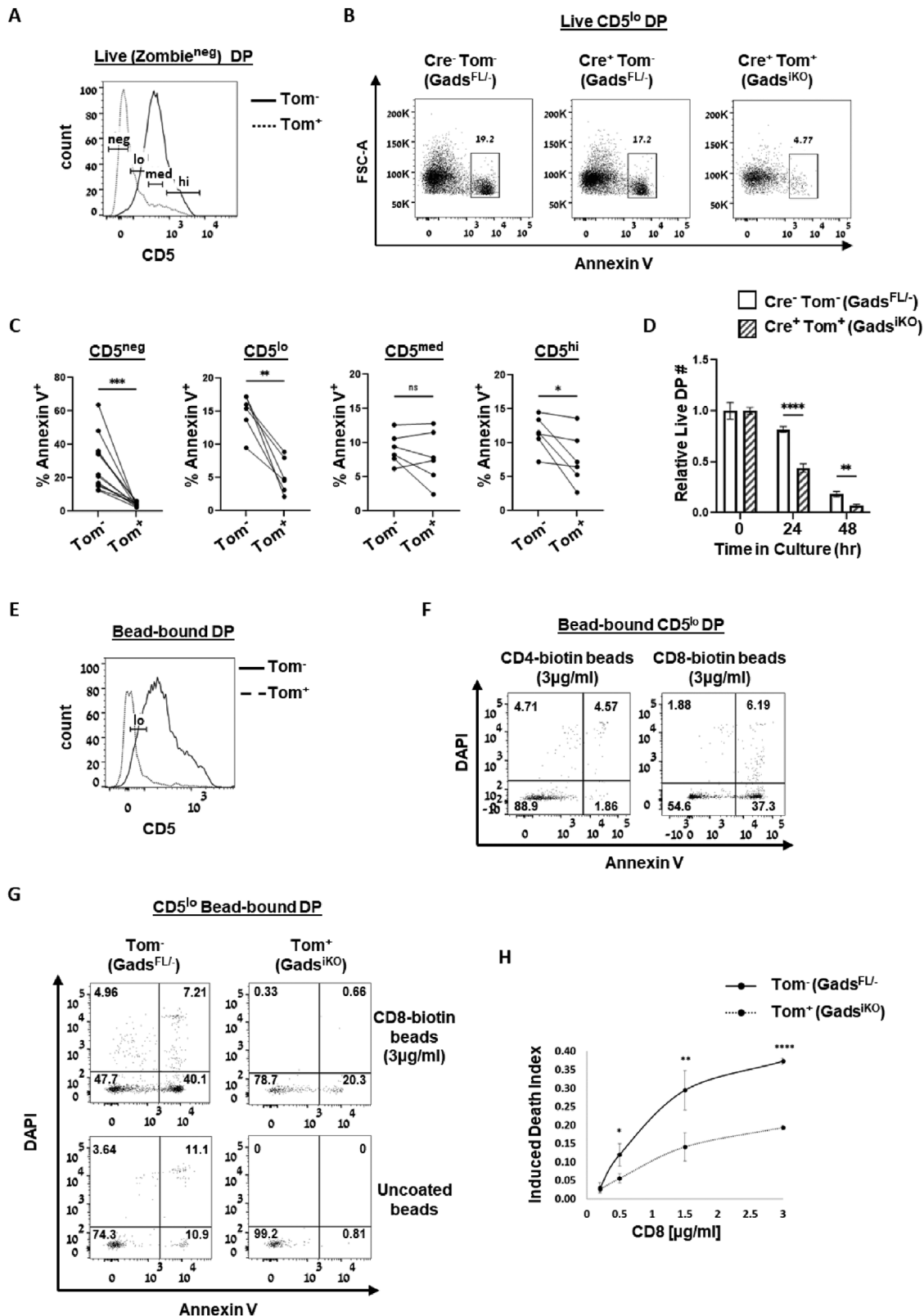


FIGURE 7 | Gads facilitates death by neglect within the unselected DP population. (A–C) in situ death within the DP compartment. Mice were harvested 2 to 2.5 weeks after starting tamoxifen. (A) CD5 expression gates were used to distinguish DP populations of interest. (B) Annexin V staining within the live CD5^{lo} DP population. Gate indicates annexin V⁺ (early apoptotic) cells. Results are representative of 8 Cre⁻ and 7 Cre⁺ mice. (C) Within-mouse comparison of early apoptotic frequency in Cre⁺, Tom⁻, and Tom⁺ DP populations of interest. Statistical significance was determined by a paired *t*-test. *n* = 6 Cre⁺ mice, within which 50–85% of DN thymocytes were Tom⁺. (D) To assess death induced by deprivation of thymus-derived survival signals, Cre⁺ and Cre⁻ total thymocytes were cultured separately. At the indicated times, live Cre⁻Tom⁻ or Cre⁺Tom⁺ DP thymocytes were identified using the gating strategy shown in Figure S2A. To calculate the relative number of live DP in each sample, we normalized the number of live DP cells to the number of reference beads in the same sample, and further normalized to time zero. Results are representative of two independent experiments.

(Figure 3C,D). Second, Gads is required to promote death by neglect in CD5^{neg-lo} DP thymocytes, both in vivo and in an ex vivo model of induced death (Figure 7). These twin defects likely explain the accumulation of CD5⁻, nonresponding, Gads^{iKO} DP thymocytes.

2.9 | Parallel Progression of Selected and Unselected Gads^{iKO} Thymocytes into the CD4 SP Compartment

To better understand the cell autonomous role of Gads in regulating thymocyte progression to the SP compartment, we performed in mouse-comparisons, using cohorts of Cre⁺ mice in which < 85% of DN thymocytes were Tom⁺. Consistent with positive selection, the vast majority of Gads-expressing CD4 SP thymocytes were found within a TCR β ^{hi}CD5^{hi} gate. (Figure 8A, left panels). Most Gads^{iKO} (Tom⁺) CD4 SP thymocytes were likewise found within the TCR β ^{hi}CD5^{hi} gate (Figure 8A, right panel). Finally, nearly all CD8 SP thymocytes, whether Gads-expressing or Gads^{iKO}, were found within the TCR β ^{hi}CD5^{hi} gate (Figure S3).

To illuminate the origins of the Gads^{iKO} TCR β ^{hi}CD5^{hi} CD4 SP population, we examined two additional markers of positive selection: increased expression of CCR7 and decreased expression of CD24 [18, 19]. Whether Gads-expressing or Gads^{iKO}, CD5⁺ CD4 SP thymocytes were found on a trajectory of increasing CCR7 and decreasing CD24, compared with the DP population from which they derived (Figure 8B, black and gray populations). In contrast, the unusual TCR β ^{lo}CD5⁻ Gads^{iKO} CD4 SP population lacked signs of positive selection, as it remained CD24^{hi} and CCR7^{lo} (Figure 8B, orange population). These markers provide additional evidence that CD5⁺ Gads^{iKO} SP thymocytes derive from TCR-driven positive selection, while a distinct subset of CD5⁻ Gads^{iKO} thymocytes progresses to the CD4 SP compartment without undergoing positive selection.

To explore the cell-autonomous role of Gads in driving each type of progression, we examined the frequency of Tom⁺ cells in the positively selected (TCR β ^{hi}CD5⁺) and unselected (TCR β ^{lo}CD5⁻) CD4 SP populations. Given the inherently chimeric nature of Gads^{iKO} mice, the frequency of Tom⁺ thymocytes should decrease as cells pass through Gads-dependent developmental junctions. The frequency of Tom⁺ cells dropped significantly, as DP cells passed into the CD5⁺ TCR β ^{hi} CD4 SP population, while increasing dramatically as cells passed into the CD5⁻ TCR β ^{lo} population; indeed, this latter population was composed almost

entirely of Tom⁺ cells (Figure 8C). Taken together our results suggest a dual function of Gads at the border between the DP and CD4 SP compartment: on the one hand, Gads is required to promote positive selection, and on the other hand, it appears to be required to prevent the developmental progression of unselected thymocytes.

Given the low TCR-responsiveness of CD5⁺ Gads^{iKO} DP cells (Figure 6G,H), the presence of positively selected Gads^{iKO} CD4 SP cells presents something of a conundrum. To address this contradiction, we sought to assess the TCR signaling competence of positively selected Gads^{iKO} CD4 SP thymocytes, by stimulating thymocytes ex vivo and measuring the induced phosphorylation of ERK, while gating on the CD5⁺ CD4 SP population. Phospho-ERK was not detected in unstimulated cells (Figure 8D, left), but was clearly detected following 2 min of stimulation with PMA and ionomycin (Figure 8D, right); moreover, the response to this stimulus was Gads-independent at all time points examined (Figure 8E, right). To induce efficient activation of the TCR signaling pathway, we co-cross-linked CD3 and CD4. At the 2 min time point, Gads expressing CD5⁺ CD4 SP cells were predominantly pERK⁺, whereas Gads^{iKO} CD5⁺ CD4 SP cells were predominantly pERK⁻ (Figure 4D, middle panel). While some degree of TCR-responsiveness was apparent, Gads^{iKO} CD5⁺ CD4 SP thymocytes exhibited markedly impaired TCR-mediated induction of pERK over the entire time course of 1–5 min of stimulation (Figure 8E, left panel). These results provide evidence for impaired TCR responsiveness, even among positively selected Gads^{iKO} thymocytes.

The weak TCR responsiveness of positively selected Gads^{iKO} CD4 SP cells raised the possibility that they may belong to the Treg lineage; however, the vast majority of positively selected Gads^{iKO} CD4 SP cells were found within the CD25⁻FoxP3⁻ (non-Treg) gate (Figure 8F). Despite a mild increase in the frequency of CD25⁺FoxP3⁺ CD4 SP thymocytes upon ablation of Gads (Figure 8G, left), their absolute number decreased (Figure 8G, right). To better understand whether Gads promotes the positive selection of Tregs, we examined the frequency of Tom⁺ cells within each compartment. To facilitate comparisons between mice, we normalized the frequency of Tom⁺ cells within each compartment to their frequency in the DP compartment of the same mouse. The frequency of Tom⁺ Tregs did not significantly differ from the frequency of Tom⁺ cells in the DP compartment of the same mouse, yet Tom⁺ cells were markedly reduced within the population of positively-selected non-Tregs (Figure 8H). These results suggest that Gads does not markedly influence the positive selection of Tregs, but is required for the positive selection of conventional CD4 SP thymocytes.

n = 4 technical repeats. Statistical significance was determined by a two-way ANOVA, Šidák's multiple comparisons test. (E–H) To assess CD8-induced apoptosis, a mixture of Tom⁺ and Tom⁻ thymocytes was incubated for 1 h at 37°C with uncoated, α CD4- or α CD8-coated beads, and then stained with cell surface markers, annexin V and DAPI. Bead-bound DP thymocytes were identified using the gating strategy shown in Figure S2B. (E) CD5^{lo} bead-bound DP cells, as defined by this gate are candidates for CD8-induced apoptosis. (F) The representative result depicts wild-type (Cre⁻Tom⁻) thymocytes within the bead-bound CD5^{lo} DP gate. Early apoptotic cells are found in the annexin V⁺ DAPI⁻ quadrant (G) Representative result within the Tom⁻ and Tom⁺ bead-bound CD5^{lo} gate. (H) Dose response of CD8-induced early apoptosis, in the presence and absence of Gads. Beads were coated with 0, 0.2, 0.5, 1.5, or 3 μ g/mL CD8-biotin. The induced death index was calculated as described in Materials and Methods. *n* = 4 technical repeats, error bars indicate standard deviation, and similar results were obtained in at least two independent experiments. Statistically significant differences between Tom⁺ and Tom⁻ samples were determined using an unpaired *t*-test.

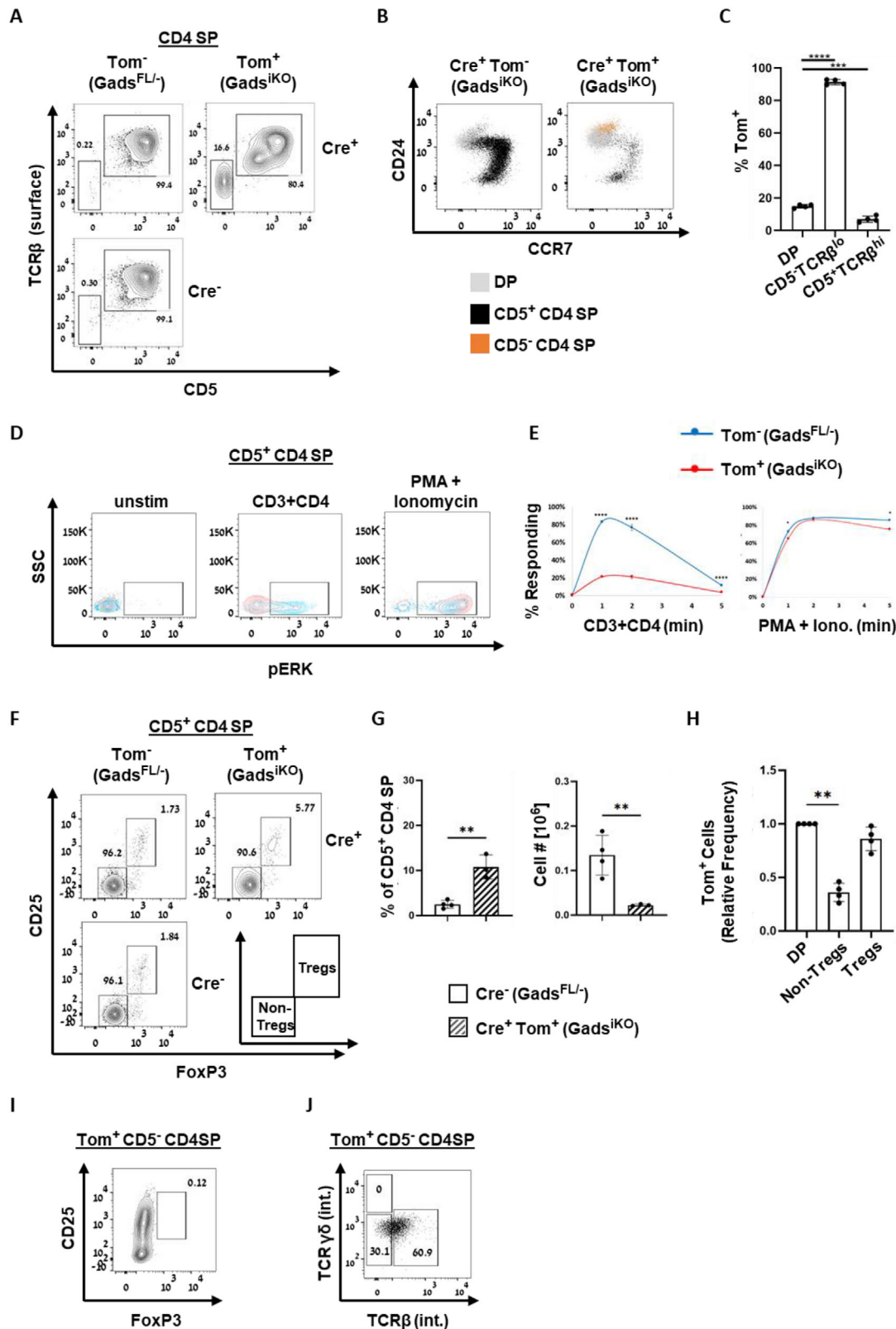


FIGURE 8 | Parallel progression of selected and unselected Gads^{iKO} thymocytes into the CD4 SP compartment. (A–C) Selected markers of positive selection within the live CD4 SP population. To exclude any potential non-SP populations from this analysis, we used a “tight” SP gate, as illustrated in Figure 2A. Thymi were harvested 2.5 weeks after starting tamoxifen treatment. (A) Representative expression of TCRβ and CD5. (B) Representative expression of CD24 and CCR7, within the indicated DP and CD4 SP subpopulations. (C) Frequency of Tom⁺ thymocytes within each of the indicated gates. $n = 4$ Cre⁺ mice, within which 50–85% of DN thymocytes were Tom⁺. Statistical significance was determined by one-way ANOVA and Dunnett’s multiple comparisons test. (D–E) TCR responsiveness of CD5⁺ CD4 SP thymocytes. Four weeks after starting tamoxifen treatment, a mixture of Tom⁺ and Tom⁻ thymocytes was stained with fluorescent surface markers and biotinylated stimulatory antibodies (CD3 and CD4), and left unstimulated or stimulated, followed by detection of pERK by intracellular staining. (D) Representative result at 2 min stimulation. Cells were unstimulated (left) or

We have not been able to definitively define the nature of the distinct CD5⁺ Gads^{iKO} CD4 SP population. These cells belong to the T cell lineage, as evidenced by their exclusion from a strict dump gate (Figure 4H) and by their intracellular expression of TCR β (Figure 4L). Yet they are not conventional SP thymocytes, as they are unselected (Figure 8B). Additional staining panels revealed that CD5⁺ Gads^{iKO} CD4 SP thymocytes do not belong to the Treg lineage (Figure 8I) nor do they belong to the TCR $\gamma\delta$ lineage (Figure 8J).

Taken together, our data demonstrate two parallel pathways of CD4 SP development in the absence of Gads. On the one hand, CD5⁺ Gads^{iKO} SP thymocytes appear to result from positive selection. On the other hand, CD5⁺ Gads^{iKO} may derive from unselected DP thymocytes that did not undergo death by neglect; rather progressing as far as the CD4 SP compartment. We do not have any evidence that this population exits the thymus, and believe it may be a “dead end” thymic population that accumulates in the absence of Gads.

3 | Discussion

Despite years of research, the regulatory roles of Gads in thymic development are not fully understood. To illuminate this issue, we developed a mouse model in which ablation of Gads is driven by a ubiquitously-expressed, tamoxifen inducible Cre recombinase, with tamoxifen administered 2–4 weeks prior to harvesting thymi. Based on this timeline, the thymic populations that we analyzed most likely derive from progenitor cells that underwent ablation of Gads prior to entering the thymus.

An important advantage of our model is that it allows in-mouse comparison of Gads-deficient and Gads-expressing thymocytes developing side by side, in a chimeric environment that is unperturbed by radiation or other dramatic treatments. Within this context, Gads-ablated thymocytes resembled germline Gads-deficient thymocytes, whereas Gads-expressing thymocytes within the same mouse phenocopied wild type thymocytes. By choosing to analyze mice in which the efficiency of recombination was 50–85%, we were able to follow the relative progression of Gads-deficient cells at any given developmental checkpoint. As thymocytes pass through Gads-dependent checkpoints, the frequency of Tom⁺ cells decreases; conversely, as cells undergo developmental transitions that are favored in the absence of Gads, the frequency of Tom⁺ cells may increase.

The marked drop in the frequency of Tom⁺ cells at the DN3 to DN4 boundary validated this approach while confirming the previously-described requirement for Gads at the β -selection checkpoint [46, 47].

Whereas Gads-deficient DN thymocytes fail to respond to anti-CD3 stimulation *in vivo* [46], this treatment does not reflect physiologic levels of stimulation. To gain further insight, we developed an approach to assess physiologic pre-TCR signaling *in vivo*, based on the established relationship between pre-TCR signaling and CD5 expression [8]. This approach revealed that Gads is required for the pre-TCR-induced increase in the expression of CD5; in contrast, as previously suggested [45], Gads was not required for δ -selection.

In addition to its role in β -selection, Gads promotes the positive and negative selection of TCR-transgenic thymocytes [46, 48]. We extended these studies to a polyclonal TCR repertoire by using CD69, TCR β and CD5 as physiologic markers of TCR-driven developmental progression *in vivo* [8, 11–13]. A substantial drop in the frequency of Tom⁺ cells at the boundary between population 3 (TCR β^{med} CD69^{med}) and population 4 (TCR β^{hi} CD69^{hi}) provides evidence for profound impairment of TCR-driven positive selection in the absence of Gads. Further supporting this conclusion, the frequency of Tom⁺ cells decreased as DP cells transited into the positively selected CD5⁺TCR β^{hi} compartment. Indeed, both the frequency and absolute number of CD5^{hi}TCR β^{hi} thymocytes profoundly decreased in the absence of Gads.

The defect in positive selection appears to originate in the DP compartment, as most Gads-deficient DP thymocytes failed to upregulate CD5, suggesting impaired TCR-mediated responsiveness to self-MHC. Nevertheless, the residual progression of CD5⁺ Gads^{iKO} thymocytes to the SP compartment suggests a degree of Gads-independent TCR responsiveness. Indeed, several lines of evidence suggest that Gads is not essential for TCR responsiveness, but rather appears to regulate the probability of response to low intensity TCR signals [39, 47, 56].

To address these issues, we assessed TCR responsiveness, while gating on potentially responsive (CD5⁺) DP and SP populations. We found that even CD5⁺ Gads^{iKO} DP thymocytes exhibited profoundly reduced TCR-induced calcium influx. Moreover, even positively selected Gads^{iKO} CD4 SP thymocytes exhibited markedly reduced TCR-induced phosphorylation of Erk. Together, these results suggest that a TCR-signaling defect under-

stimulated with 25 $\mu\text{g}/\text{mL}$ streptavidin to co-cross link CD3 and CD4 (middle) or PMA and ionomycin to bypass TCR-proximal signaling events (right). (E) Frequency of pERK⁺, CD5⁺ CD4 SP thymocytes following stimulation for 1–5 min with CD3+CD4 cross-linking (left) or PMA and ionomycin (right). Statistically significant differences between Tom⁺ and Tom⁺ cells were determined by unpaired two-tailed *t*-test. Error bars were too small to depict. This experiment was done twice in triplicates with similar results. (F–I) Treg (CD25⁺ FoxP3⁺) abundance within the CD4 SP population. Thymi were harvested 2.5–3.5 weeks after starting tamoxifen treatment. (F) Representative expression of CD25 and Foxp3 within the CD5⁺ CD4⁺ SP population. Populations of interest are defined at the bottom right. (G) Frequency (left) and absolute number (right) of Treg cells within the CD5⁺ CD4⁺ SP population. Statistical significance was determined by unpaired *t*-test. *n* = 4 Cre⁺ and a cohort of 3 Cre⁺ mice with >95% Tom⁺ PBLs. (H) The frequency of Tom⁺ thymocytes within each of the indicated populations of interest. To facilitate statistically valid comparisons between mice, the frequency of Tom⁺ cells in each gate was normalized to their frequency in the DP compartment of the same mouse. Statistical significance was determined by a one-way ANOVA, Dunnett's multiple comparisons test. *n* = 4 Cre⁺ mice, with 70–90% Tom⁺ PBLs. (I) Representative expression of CD25 and Foxp3 within the Tom⁺ CD5⁺ CD4⁺ SP population. (J) Representative intracellular staining for the β - and $\gamma\delta$ -TCR, within the Tom⁺ CD5⁺ CD4⁺ SP population, while employing a dump gate (anti-mouse NK1.1, CD8 α , TER-119, Gr-1, CD11b, and B220) to exclude CD8⁺ and NK1.1⁺ thymocytes, and non-T cell lineages, as in Figure 4.

lies the impairment of positive selection in Gads-deficient DP thymocytes.

The observed pre-TCR and TCR signaling defects likely reflect the role of Gads in mediating the TCR-induced recruitment of SLP-76 to LAT. This task is facilitated by the high affinity (low nanomolar) constitutive binding of Gads to SLP-76 [32]. Grb2 most likely cannot compensate for Gads, since its binding to SLP-76 occurs at 1000-fold lower affinity [32]. Thus, TCR-induced recruitment of SLP-76 to LAT is profoundly reduced in the absence of Gads, but is not affected by deletion of other Grb2-family members [39, 57].

Despite the dual impairment of β - and positive selection, unselected thymocytes progressed as far as the CD4 compartment. This aberrant phenomenon was observed using two different definitions of unselected thymocytes: TCR β ⁺CD69⁺ and CD5⁺TCR β ⁺. Both the frequency and number of unselected CD4 SP thymocytes far surpassed their prevalence among Gads-expressing thymocytes; indeed, this population was composed almost exclusively of Tom⁺ cells. To rule out the inclusion of transitional cells in our analyses, throughout this study, we defined CD4 SP cells using a “tight” CD4^{hi} CD8^{neg} gate, as illustrated in Figure 2A.

This population of CD5⁺TCR β ⁺ Gads^{iKO}, unselected CD4 SP thymocytes did not include $\gamma\delta$ or Treg cells, and lacked markers of positive selection, as the cells remained in an immature, CD24^{hi}TCR β ^{lo}CCR7^{lo} state. Surprisingly, the cells tended to express CD25; thus, resembling DN thymocytes undergoing β -selection.

The CD5⁺ Gads^{iKO} CD4 SP population likely corresponds to the CD24^{hi}TCR β ^{lo} CD4 SP population that accumulates in TCR-transgenic Gads-deficient mice [48]. A population of CD24^{hi} CD8 SP thymocytes was likewise observed in cyclosporin A-treated HY-transgenic female mice [58]. Together, these results suggest that upon partial disruption of TCR signaling, unselected thymocytes may advance to the SP compartments, while failing to mature. Although Dalheimer et al. [48] interpreted their results as an uncoupling of positive selection from developmental progression, we suggest that a failure of death by neglect may underlie the aberrant developmental progression of Gads-deficient cells to the CD4 compartment, in the absence of both β - and positive-selection.

The reduced TCR signaling competence of Gads-deficient DP thymocytes should result in a corresponding increase in death by neglect, which occurs in MHC-nonresponsive wild-type thymocytes [14, 15]. Consistent with this expectation, Gads^{iKO} thymocytes underwent efficient apoptosis in tissue culture, a common model for death by neglect. Yet, CD5⁺ Gads^{iKO} DP thymocytes accumulated in vivo, in both the inducible and the germline Gads-deficient models. This previously unreported phenotype first suggested to us that Gads might be required to induce the death of MHC-nonresponding DP thymocytes in situ. This notion is supported by the reduced frequency of annexin V⁺ cells among CD5^{neg-lo} Gads^{iKO} DP thymocytes.

Taken alone, the reduced frequency of death by neglect in situ is difficult to interpret. One possibility is that, in the absence

of Gads, TCR signaling may be reduced to a level that is sufficient for survival but insufficient for efficient positive selection. Alternatively, our results may suggest a novel reinterpretation of the process of death by neglect. Rather than constituting a passive response to the absence of signaling events, the death of MHC-nonresponsive DP thymocytes may be actively induced by particular signaling pathways that depend on Gads. In particular, it is possible that β -selection triggers a “time bomb” that induces death within a certain time frame unless cells are rescued by positive selection. Gads may be somehow required to trigger this β -selection-associated death clock.

The notion that T cell-specific signaling pathways may be involved in triggering death by neglect was first suggested by Grebe et al. [55], who demonstrated that cross-linking of CD8 induced apoptotic death, specifically in CD5^{lo}, but not in CD5^{hi} DP thymocytes. This death could be prevented by co-crosslinking CD8 and CD3 [55]. Based on these results Grebe et al. [55] suggested that CD5^{lo} DP thymocytes are able to detect signaling through CD8 and that in the absence of concomitant signaling through the TCR, the CD8-induced signaling pathway can trigger a form of death that may be related to the phenomenon of death by neglect. In support of their hypothesis, they note that early DP thymocytes express a nonsialylated form of CD8, that binds with high affinity to class I MHC [59, 60], and therefore may be able to induce signaling events in the absence of TCR ligation.

We recapitulated the observation of CD8-induced death of CD5^{lo} DP thymocytes, moreover, we extended this system to show that death is specifically induced by ligation CD8, but not CD4. Most importantly, we showed that Gads is required for optimal CD8-induced death in this experimental model. These findings suggest the possibility that, in addition to its role in mediating TCR signaling, Gads may participate in a CD8-induced signaling pathway.

To the best of our knowledge, our observation provides the first evidence that signaling elements downstream of the TCR may be involved in triggering the death of TCR-nonresponsive DP thymocytes. Perhaps consistent with an involvement of Gads in cell death, Gads contains a caspase 3 cleavage site [61, 62]; moreover, Gads-deficient T1 B cells were shown to be resistant to BCR-induced apoptosis [63]. Taken together, our results suggest a new paradigm in which Gads regulates the balance between positive selection and death by neglect. Both processes are reduced in the absence of Gads, resulting in the survival and developmental progression of unselected thymocytes.

3.1 | Data Limitations and Perspectives

This study provides preliminary validation of a new mouse model for studying Gads. The model provides a number of advantages for future studies, first because of its intrinsically chimeric nature, and second because it will provide a way to characterize the role of Gads in developmentally normal T cells.

Gads is strongly implicated in the Fc ϵ Ri signaling pathway [35, 64], which plays an important role in type I allergic responses, yet the development of Gads as a drug target has been hampered by a lack of knowledge about the implications of Gads inhibition in

developmentally-normal mature T cells. Germline Gads-deficient mice are not suitable for this purpose, as they produce nonnaïve, innate-like peripheral T cells [47]; moreover, the TCR repertoire of positively selected Gads-deficient thymocytes may be skewed toward higher affinity receptors that are uniquely capable of signaling in the absence of Gads. We expect that the model described here will provide an appropriate experimental system for addressing these questions.

4 | Materials and Methods

4.1 | Antibodies and Staining Reagents

Anti-mouse antibodies CD4-PerCP-Cy5.5, or -FITC, or -APC-Cy7 (Clone RM4-4 and GK1.5), CD8a-APC-Cy7, or -APC, or -FITC (Clone 53-6.7 or QA17A07), CD44-BV421 (Clone IM7), CD5-BV711 (Clone 53-7.3), CD25-APC (Clone PC61), NK1.1-FITC (Clone PK136), TCR γ/δ -FITC, or -PerCP-Cy5.5 (Clone GL3), TCR β chain-BV605, or -PE-Cy7 (Clone H57-597), CD69-KB520 (clone H1.2F3), FOXP3-AF488 (clone MF-14), pERK1/2 (T204/Y202)-APC (clone MILAN8R), CD24-APC (clone M1/69), CD197 (CCR7)-AF488 (Clone 4B12), Ly-6G/Ly-6C (Gr-1)-FITC (clone RB6-8C5), CD45R/B220-FITC (clone RA3-6B2), TER-119/erythroid cells-FITC (clone TER-119), CD11b-FITC (clone M1/70), Fc ϵ R1 α -FITC (clone MAR-1), CD11c-FITC (clone N418), CD19-FITC (clone 1D3/CD19), Zombie Aqua Fixable viability kit (BioLegend, 423101), isotype control antibodies Armenian hamster IgG-FITC, rat IgG2a, κ -FITC, rat IgG2b, κ -FITC, mouse IgG2a, κ -FITC and Armenian hamster IgG- PE/Cy7, and biotin-conjugated anti-mouse CD3 ϵ (clone145-2C11), CD4 (clone RM4-4) and CD8 (clone 53-6.7) were from Biolegend. Cleaved caspase 3-AF647 (Clone D3E9) was from Cell Signaling. Gads-AF647 (UW40) was from Santa Cruz Biotechnology. Unless noted otherwise, all PBS used in this study is without calcium and magnesium.

4.2 | Mice

Mice were on the C57BL/6 background. Gads-deficient (Gads^{-/-}) mice [46] were generously provided by C. Jane McGlade (University of Toronto). Gads^{FL} mice, in which LoxP signals flank Grap2 (Gads) exon2, were generated for us by Cyagen/Taconic, by using CRISPR/Cas9-mediated genome engineering on the C57BL/6 background, to insert LoxP sites into the introns that flank Grap2 exon 2 on chromosome 15. This modification permits Cre-mediated deletion of a 592 bp region, including Grap2 exon 2. gRNA sequences were GCGCATCTAAGGAGGCCGAGGG and CCTATAACGAATGCAGTTGCAGG. The targeting vector was generated by PCR using BAC clones RP23-61M17 and RP23-453G11 from the C57BL/6 library as template. The insertion was verified in F1 mice by southern blotting and by sequencing the intended target site. To eliminate potential off target effects, the five most-likely off target sites were sequenced. F1 Gads^{FL} mice were backcrossed once onto the C57BL/6 background, and further backcrossed during the course of cross-breeding to Jackson Laboratory strain #007914 (Ai14), to incorporate a Cre-dependent tdTomato (Tom^{FL-stop}) reporter at the Rosa26 locus [49]. The ubiquitously-expressed, tamoxifen-inducible UBC-Cre-ERT2 Cre recombinase [50] was maintained in a hemizygous

state. To generate mice for experiments, Gads^{FL/FL}Tom^{FL-stop/FL-stop} mice were bred to Gads-deficient Cre driver mice (Gads^{-/-}UBC-Cre-ERT2⁺), to generate Gads^{FL/-}Tom^{FL-stop} progeny, either Cre⁺ or Cre⁻.

4.3 | Tamoxifen-Inducible Deletion of Gads

Tamoxifen (Sigma, T5648) was dissolved at 10 mg/ml in fresh corn oil by shaking at 37°C for 3–4 h. For tamoxifen-inducible deletion of Gads, 6–7-week-old Gads^{FL/-}Tom^{FL-stop} mice, either UBC-Cre-ERT2⁺ or Cre⁻, were treated with tamoxifen daily for five days by intraperitoneal injection (75 μ g/g mouse weight). To assess the efficiency of Cre-mediated recombination, 200 μ l of blood was collected from the cheek into 1.5 mL Eppendorf tubes containing 50 units of heparin. Blood samples were diluted to 2 mL in PBS and underlaid with 2 mL of Histopaque-1083 (Sigma, 10831). Following centrifugation at 400 g for 30 min at room temperature, leukocytes were collected from the interface, and washed once in PBS and once in FACS buffer, prior to staining for flow cytometry.

4.4 | Thymocyte Isolation and Staining

A single-cell suspension of thymocytes was generated by pressing the thymus through a 40 μ m Cell Strainer. Cells were washed once with PBS supplemented with 2% FCS, PenStrep (Sartorius, 03-031-1B), and 1 mM EDTA, then washed and re-suspended in 10 mL PBS without FCS. Cells were stained for 30 min at RT in the dark with Zombie Aqua Fixable Viability Kit. Staining was terminated by washing cells with 2 mL FACS buffer (PBS, supplemented with 2% FCS and 0.02% sodium azide). Cells were then stained for 15–30 min at 4°C with a cocktail of fluorescently labeled antibodies in FACS buffer, and processed as indicated below. In most cases, stained cells were washed once with FACS buffer and once with PBS, fixed for 20–40 min at RT in the dark with a 1:1 dilution of fixation buffer in PBS (IC Fixation Buffer Thermo Fischer Scientific, 00-8222-49), then washed in FACS buffer. For intracellular staining of Gads or TCR, fixed cells were washed twice with 1 \times Thermo Fischer Scientific permeabilization buffer (Invitrogen, 00-8333-56), prior to intracellular staining in the same buffer. For intracellular staining with FOXP3, we used the True Nuclear Transcription Factor Buffer set (Biolegend 424401). Where indicated, unfixed, stained cells were washed with Annexin V Binding Buffer (Biolegend, 422201), stained for 15 min at RT with annexin V-APC (Biolegend, 640919), and then read immediately by flow cytometry.

4.5 | Flow Cytometry

Stained cells were read on a Fortessa II flow cytometer, using single-stained cells or compensation beads as controls. Results were analyzed with FlowJo Software while gating on live (Zombie-negative) single cells. When indicated in figure legends, a FITC-labeled dump gate was used to exclude some or all of the following: NK1.1⁺, TCR $\gamma\delta$ ⁺, and/or CD8⁺ T cells, as well as cells that stained positive for Ly-6G/Ly-6C (Gr-1), CD45R/B220, TER-119, CD11b, Fc ϵ R1 α , CD11c, and CD19.

4.6 | Ex Vivo Models of Death by Neglect

Freshly isolated thymocytes were resuspended in Hepes-buffered complete T cell medium (high glucose DMEM, supplemented with 10% iron-fortified bovine calf serum, NEAA (nonessential amino acids), 2 mM glutamax, 1 mM sodium pyruvate, 50 μ M β -mercaptoethanol, pen-strep, and 20 mM Hepes, pH7.3).

To assess CD8-induced death, avidin beads (Spherotech, SVP-30-5) were preincubated with different concentrations of CD4- or CD8-biotin, then washed and resuspended in a Hepes-buffered complete T cell medium. To induce death, 0.25×10^6 thymocytes were preincubated at 37°C for 15 min and then mixed in a round-bottomed well with 1.25×10^6 precoated avidin beads. After incubation at 37°C for 1 h, the cells were washed once with cold FACS buffer, stained at 4°C with surface antibodies for CD4, CD8, and CD5, washed once with FACS buffer and once with annexin V binding buffer, and stained for 15 min at RT with annexin V and DAPI. To calculate the induced death index, the net CD8-induced increase in the early apoptotic population was expressed as a fraction of the population that was live at baseline ($(\% \text{annexinV}^+ \text{DAPI}^-_{\text{exp}} - \% \text{annexinV}^+ \text{DAPI}^-_{\text{baseline}}) / \% \text{annexinV}^- \text{DAPI}^-_{\text{baseline}}$).

To assess death induced by deprivation of thymus-derived survival signals, thymocytes were mixed with a fixed amount of PKH26 reference microbeads (Sigma-Aldrich P7458), aliquoted to flat-bottomed tissue culture wells, and incubated at 37°C and 10% CO₂. At the indicated times, cells and beads from individual wells were collected, washed once with PBS, and stained with Zombie Aqua Fixable Viability Kit, followed by staining with surface antibodies and fixation with IC Fixation Buffer Thermo Fischer Scientific. Live (Zombie^{neg}) Tom⁺ or Tom⁻ DP cells were counted by flow cytometry while normalizing to the number of PKH26 reference beads counted in the same tube.

4.7 | Calcium Fluorimetry

Calcium flux was measured using a mixture of thymocytes from tamoxifen-treated Cre⁺ and Cre⁻ mice. Thymocytes were washed with calcium staining buffer (RPMI supplemented with 1% FCS, 20 mM Hepes pH 7.3, and 2 mM glutamine), and incubated in the dark for 30 min at 30°C, with 0.5 mL per each 5 million cells of calcium staining buffer containing 4 μ M indo-1 AM (eBioscience), 2 mM probenecid, fluorescent cell surface markers, including CD4-FITC (clone GK1.5) and CD8-APC (clone QA17A07), and biotinylated stimulatory antibodies: CD3, CD4 (clone RM4-4) and CD8 (clone 53-6.7), 3 μ g/mL each. The stained cells were then washed twice and resuspended in RPMI supplemented 20 mM Hepes pH 7.3, and 2 mM Glutamine. Cells were stored on ice and preheated to 37°C for 5 min prior to ratiometric calcium fluorimetry, which was performed by flow cytometry, with the temperature maintained at 37°C, and stimulation was induced at the 60 s time point by adding streptavidin (Biolegend, 405150) to a final concentration of 25 μ g/mL, or ionomycin to a final concentration of 1 μ M. Excitation was at 355 nm and emission was measured using the bandpass filters 405/20 (Ca-bound indo-1) and 485/22 (free indo-1), with data presented as the ratio between these two values. Data analysis was performed while gating on CD5⁺, Tom⁺, or Tom⁻ DP thymocytes.

4.8 | TCR-Induced ERK Phosphorylation

A mixture of thymocytes from tamoxifen-treated Cre⁺ and Cre⁻ mice was washed with calcium staining buffer and stained with cell surface markers for 15 min at 4°C in the same buffer. Staining antibodies included CD4-FITC (clone GK1.5), CD8-APC-Cy7 (clone 53-6.7), CD5-BV711 (clone 53-7.3), along with 3 μ g/mL each of the biotinylated stimulatory antibodies: CD3 (clone 2C11) and CD4 (clone RMA 4-4). The stained cells were washed twice and re-suspended in stimulation buffer (RPMI with 20 mM Hepes pH 7.3, and 2 mM Glutamine), and were preheated to 37°C for 10 min prior to stimulation. TCR stimulation was induced by adding streptavidin to a final concentration of 25 μ g/mL and was terminated by the addition of an equal volume of IC Fixation Buffer (Thermo Fischer Scientific) and incubated for 30 min at RT, then cells were washed with FACS buffer and stored at 4°C. Permeabilization was performed by resuspending the cell pellet in cold 100% methanol, after incubation for 1hr on ice, cells were washed with FACS buffer and stained with phospho-ERK antibody for 30 min at RT. Phospho-ERK staining was evaluated by flow cytometry while gating on CD5⁺ CD4 SP thymocytes.

4.9 | Statistical Analysis

All experiments in this study were performed two or more times with similar results. Statistical analysis was performed using the Prism software package. *p*-values were determined using the statistical tests indicated in figure legends. The following symbols were used to indicate statistically significant *p*-values: **p* < 0.05; ***p* < 0.01; ****p* < 0.001; *****p* < 0.0001.

Author Contributions

Rose Shalah and Deborah Yablonski developed the study objectives and experimental strategy with key inputs from Manal Marzouk and Enas Hallumi. Rose Shalah and Manal Marzouk performed experiments, analyzed data and prepared the figures. Naama Klopstock designed and carried out all breeding and genotyping strategies for these experiments. This manuscript was written by Deborah Yablonski, Rose Shalah, and Manal Marzouk. All authors have read and agreed to the published version of the manuscript.

Acknowledgments

This research was supported by grants to Deborah Yablonski from the Israel Science Foundation (283/22), the Rappaport Family Institute for Research in the Medical Sciences, the Minerva Stiftung Center Programme on Cell Intelligence, and the Colleck Research Fund. The Biomedical Core Facility (BCF) of the Rappaport Faculty of Medicine provided access to flow cytometry equipment. We thank BCF staff members Ofer Shenker, Amir Grau, Rotem Honen Kadosh and Jeeda Bisharat for providing excellent technical support and Ido Griness from the Technion Statistics Lab for his welcome advice on statistical analyses. Gads-deficient mice were generously provided by C. Jane McGlade (University of Toronto). We thank our chief veterinarians Dr. Rona Shofti and Dr. Dvir Mintz, as well as Paul Zannou, Olga Ugortsin and the rest of the excellent staff from the Technion Preclinical Authority for professional assistance with the care, treatment and housing of the mice. Pamela Schwartzberg and Dominic Golec from the NIH/NIAID and Leslie Berg from the University of Colorado provided much appreciated input into the interpretation of thymic phenotypes.

Ethics Approval Statement

All mice were maintained in an SPF facility under veterinary supervision and in accordance with institutional ethics guidelines. All experiments using animals were done with the permission of our national and local authorities. All authors were trained and certified to conduct experiments in rodents at the Technion.

Conflicts of Interest

The authors declare no conflicts of interest. The funders of this study had no role in the design of the study, in the collection, analyses, or interpretation of data, in the writing of the manuscript, or in the decision to publish the results.

Data Availability Statement

The data that support the findings of this study are available from the corresponding author upon reasonable request.

Peer Review

The peer review history for this article is available at <https://publons.com/publon/10.1002/eji.202451000>.

References

1. G. P. Morris and P. M. Allen, "How the TCR Balances Sensitivity and Specificity for the Recognition of Self and Pathogens," *Nature Immunology* 13, no. 2 (2012): 121–128.
2. A. E. Moran and K. A. Hogquist, "T-Cell Receptor Affinity in Thymic Development," *Immunology* 135, no. 4 (2012): 261–267.
3. G. Fu, V. Rybakina, J. Brzostek, W. Paster, O. Acuto, and N. R. J. Gascoigne, "Fine-Tuning T Cell Receptor Signaling to Control T Cell Development," *Trends in Immunology* 35, no. 7 (2014): 311–318.
4. K. A. Hogquist and S. C. Jameson, "The Self-Obsession of T Cells: How TCR Signaling Thresholds Affect Fate 'Decisions' and Effector Function," *Nature Immunology* 15, no. 9 (2014): 815–823.
5. D. I. Godfrey, J. Kennedy, T. Suda, and A. Zlotnik, "A Developmental Pathway Involving Four Phenotypically and Functionally Distinct Subsets of CD3-CD4-CD8- Triple-Negative Adult Mouse Thymocytes Defined by CD44 and CD25 Expression," *The Journal of Immunology* 150, no. 10 (1993): 4244–4252.
6. I. Aifantis, M. Mandal, K. Sawai, A. Ferrando, and T. Vilimas, "Regulation of T-Cell Progenitor Survival and Cell-Cycle Entry by the Pre-T-Cell Receptor," *Immunological Reviews* 209, no. 1 (2006): 159–169.
7. I. Aifantis, F. Gounari, L. Scorrano, C. Borowski, and H. von Boehmer, "Constitutive Pre-TCR Signaling Promotes Differentiation Through Ca2+ Mobilization and Activation of NF- κ B and NFAT," *Nature Immunology* 2, no. 5 (2001): 403–409.
8. H. S. Azzam, A. Grinberg, K. Lui, H. Shen, E. W. Shores, and P. E. Love, "CD5 Expression Is Developmentally Regulated by T Cell Receptor (TCR) Signals and TCR Avidity," *Journal of Experimental Medicine* 188, no. 12 (1998): 2301–2311.
9. L. Passoni, E. S. Hoffman, S. Kim, et al., "Intrathymic Delta Selection Events in Gammadelta Cell Development," *Immunity* 7, no. 1 (1997): 83–95.
10. R. Muro, H. Takayanagi, and T. Nitta, "T Cell Receptor Signaling for $\gamma\delta$ T Cell Development," *Inflammation and Regeneration* 39, no. 1 (2019): 6.
11. E. R. Breed, M. Watanabe, and K. A. Hogquist, "Measuring Thymic Clonal Deletion at the Population Level," *Journal of Immunology* 202, no. 11 (2019): 3226–3233.
12. G. Fu, S. Vallee, V. Rybakina, et al., "Themis Controls Thymocyte Selection Through Regulation of T Cell Antigen Receptor-Mediated Signaling," *Nature Immunology* 10, no. 8 (2009): 848–856.
13. B. B. Au-Yeung, H. J. Melichar, J. O. Ross, et al., "Quantitative and Temporal Requirements Revealed for Zap70 Catalytic Activity During T Cell Development," *Nature Immunology* 15, no. 7 (2014): 687–694.
14. C. D. Surh and J. Sprent, "T-Cell Apoptosis Detected in Situ During Positive and Negative Selection in the thymus," *Nature* 372, no. 6501 (1994): 100–103.
15. Z. Szondy, É. Garabuczi, K. Tóth, B. Kiss, and K. Köröskényi, "Thymocyte Death by Neglect: Contribution of Engulfing Macrophages," *European Journal of Immunology* 42, no. 7 (2012): 1662–1667.
16. M. Merkenschlager, D. Graf, M. Lovatt, U. Bommhardt, R. Zamoyska, and A. G. Fisher, "How Many Thymocytes Audition for Selection?," *Journal of Experimental Medicine* 186, no. 7 (1997): 1149–1158.
17. M. A. Daniels, E. Teixeira, J. Gill, et al., "Thymic Selection Threshold Defined by Compartmentalization of Ras/MAPK Signalling," *Nature* 444, no. 7120 (2006): 724–729.
18. M. A. Weinreich and K. A. Hogquist, "Thymic Emigration: When and How T Cells Leave Home," *Journal of Immunology* 181, no. 4 (2008): 2265–2270.
19. C. M. Witt and E. A. Robey, "The Ins and Outs of CCR7 in the thymus," *Journal of Experimental Medicine* 200, no. 4 (2004): 405–409.
20. R. J. Brownlie and R. Zamoyska, "T Cell Receptor Signalling Networks: Branched, Diversified and Bounded," *Nature Reviews Immunology* 13, no. 4 (2013): 257–269.
21. A. K. Chakraborty and A. Weiss, "Insights Into the Initiation of TCR Signaling," *Nature Immunology* 15, no. 9 (2014): 798–807.
22. J. Lin and A. Weiss, "Identification of the Minimal Tyrosine Residues Required for Linker for Activation of T Cell Function," *Journal of Biological Chemistry* 276, no. 31 (2001): 29588–29595.
23. P. E. Paz, S. Wang, H. Clarke, X. Lu, D. Stokoe, and A. Abo, "Mapping the Zap-70 Phosphorylation Sites on LAT (linker for activation of T cells) Required for Recruitment and Activation of Signalling Proteins in T Cells," *Biochemical Journal* 356, no. Pt 2 (2001): 461–471.
24. W. Zhang, R. P. Tribble, M. Zhu, S. K. Liu, C. J. McGlade, and L. E. Samelson, "Association of Grb2, Gads and Phospholipase C- β 1 With Phosphorylated LAT Tyrosine Residues," *Journal of Biological Chemistry* 275, no. 30 (2000): 23355–23361.
25. M. Zhu, E. Janssen, and W. Zhang, "Minimal Requirement of Tyrosine Residues of Linker for Activation of T Cells in TCR Signaling and Thymocyte Development," *Journal of Immunology* 170, no. 1 (2003): 325–333.
26. J. B. Wardenburg, C. Fu, J. K. Jackman, et al., "Phosphorylation of SLP-76 by the ZAP-70 Protein-Tyrosine Kinase Is Required for T-Cell Receptor Function," *Journal of Biological Chemistry* 271, no. 33 (1996): 19641–19644.
27. N. Fang, D. G. Motto, S. E. Ross, and G. A. Koretzky, "Tyrosines 113, 128, and 145 of SLP-76 Are Required for Optimal Augmentation of NFAT Promoter Activity," *Journal of Immunology* 157 (1996): 3769–3773.
28. M. Sela, Y. Bogin, D. Beach, et al., "Sequential Phosphorylation of SLP-76 at Tyrosine 173 Is Required for Activation of T and Mast Cells," *The EMBO Journal* 30, no. 15 (2011): 3160–3172.
29. L. Balagopalan, N. P. Coussens, E. Sherman, L. E. Samelson, and C. L. Sommers, "The LAT Story: A Tale of Cooperativity, Coordination, and Choreography," *Cold Spring Harbor Perspectives in Biology* 2, no. 8 (2010): a005512.
30. G. A. Koretzky, F. Abtahian, and M. A. Silverman, "SLP76 and SLP65: Complex Regulation of Signalling in Lymphocytes and Beyond," *Nature Reviews Immunology* 6 (2006): 67–78.
31. D. Yablonski, "Bridging the Gap: Modulatory Roles of the Grb2-Family Adaptor, Gads, in Cellular and Allergic Immune Responses," *Frontiers in Immunology* 10, no. 1704 (2019), <https://doi.org/10.3389/fimmu.2019.01704>.
32. B. T. Seet, D. M. Berry, J. S. Maltzman, et al., "Efficient T-Cell Receptor Signaling Requires a High-Affinity Interaction Between the Gads C-SH3

- Domain and the SLP-76 RxxK Motif," *The EMBO Journal* 26, no. 3 (2007): 678–689.
33. J. C. Houtman, Y. Higashimoto, N. Dimasi, et al., "Binding Specificity of Multiprotein Signaling Complexes Is Determined by both Cooperative Interactions and Affinity Preferences," *Biochemistry* 43, no. 14 (2004): 4170–4178.
 34. Q. Liu, D. Berry, P. Nash, T. Pawson, C. J. McGlade, and S. S. Li, "Structural Basis for Specific Binding of the Gads SH3 Domain to an RxxK Motif-Containing SLP-76 Peptide: A Novel Mode of Peptide Recognition," *Molecular Cell* 11, no. 2 (2003): 471–481.
 35. S. Sukenik, M. P. Frushicheva, C. Waknin-Lellouche, et al., "Dimerization of the Adaptor Gads Facilitates Antigen Receptor Signaling by Promoting the Cooperative Binding of Gads to the Adaptor LAT," *Science signaling* 10, no. 498 (2017): eaal1482.
 36. H. Asada, N. Ishii, Y. Sasaki, et al., "Grf40, a Novel Grb2 family Member, Is Involved in T Cell Signaling Through Interactions With SLP-76 and LAT," *Journal of Experimental Medicine* 189, no. 9 (1999): 1383–1390.
 37. C.-L. Law, M. K. Ewings, P. M. Chaudhary, et al., "GrpL, a Grb2-Related Adaptor Protein, Interacts With SLP-76 to Regulate Nuclear Factor of Activated T Cell Activation," *Journal of Experimental Medicine* 189, no. 8 (1999): 1243–1253.
 38. S. K. Liu, N. Fang, G. A. Koretzky, and C. J. McGlade, "The Hematopoietic-Specific Adaptor Protein Gads Functions in T-Cell Signaling via Interactions With the SLP-76 and LAT Adaptors," *Current Biology* 9 (1999): 67–75.
 39. J. Lugassy, J. Corso, D. Beach, et al., "Modulation of TCR Responsiveness by the Grb2-Family Adaptor," *Gads Cell Signal* 27, no. 1 (2015): 125–134.
 40. M. Y. Bilal, E. Y. Zhang, B. Dinkel, D. Hardy, T. M. Yankee, and J. C. Houtman, "GADS Is Required for TCR-Mediated Calcium Influx and Cytokine Release, but Not Cellular Adhesion, in human T Cells," *Cell Signalling* 27, no. 4 (2015): 841–850.
 41. M. S. Jordan and G. A. Koretzky, "Coordination of Receptor Signaling in Multiple Hematopoietic Cell Lineages by the Adaptor Protein SLP-76," *Cold Spring Harbor perspectives in biology* 2, no. 4 (2010): a002501.
 42. J. L. Clements, B. Yang, S. E. Ross-Barta, et al., "Requirement for the Leukocyte-Specific Adapter Protein SLP-76 for Normal T Cell Development," *Science* 281 (1998): 416–419.
 43. V. Pivniouk, E. Tsitsikov, P. Swinton, G. Rathbun, F. W. Alt, and R. S. Geha, "Impaired Viability and Profound Block in Thymocyte Development in Mice Lacking the Adaptor Protein SLP-76," *Cell* 94 (1998): 229–238.
 44. W. Zhang, C. L. Sommers, D. N. Burshtyn, et al., "Essential Role of LAT in T Cell Development," *Immunity* 10 (1999): 323–332.
 45. L. Zeng, S. L. Dalheimer, and T. M. Yankee, "Gads-/- mice Reveal Functionally Distinct Subsets of TCRbeta+ CD4-CD8- Double-Negative Thymocytes," *Journal of Immunology* 179, no. 2 (2007): 1013–1021.
 46. J. Yoder, C. Pham, Y.-M. Iizuka, et al., "Requirement for the SLP-76 Adaptor GADS in T Cell Development," *Science* 291 (2001): 1987–1991.
 47. T. M. Yankee, T. J. Yun, K. E. Draves, et al., "The Gads (GrpL) Adaptor Protein Regulates T Cell Homeostasis," *Journal of Immunology* 173, no. 3 (2004): 1711–1720.
 48. S. L. Dalheimer, L. Zeng, K. E. Draves, et al., "Gads-Deficient Thymocytes Are Blocked at the Transitional Single Positive CD4+ Stage," *European Journal of Immunology* 39, no. 5 (2009): 1395–1404.
 49. L. Madisen, T. A. Zwingman, S. M. Sunkin, et al., "A Robust and High-Throughput Cre Reporting and Characterization System for the Whole Mouse Brain," *Nature Neuroscience* 13, no. 1 (2010): 133–140.
 50. Y. Ruzankina, C. Pinzon-Guzman, A. Asare, et al., "Deletion of the Developmentally Essential Gene *ATR* in Adult Mice Leads to Age-Related Phenotypes and Stem Cell Loss," *Cell Stem Cell* 1, no. 1 (2007): 113–126.
 51. K. Shortman and L. Wu, "Early T Lymphocyte Progenitors," *Annual Review of Immunology* 14 (1996): 29–47.
 52. K. Kikuchi, Y. Kawasaki, N. Ishii, et al., "Suppression of Thymic Development by the Dominant-Negative Form of Gads," *International Immunology* 13, no. 6 (2001): 777–783.
 53. M. Saini, C. Sinclair, D. Marshall, M. Tolaini, S. Sakaguchi, and B. Seddon, "Regulation of *Zap70* Expression during Thymocyte Development Enables Temporal Separation of CD4 and CD8 Repertoire Selection at Different Signaling Thresholds," *Science Signaling* 3, no. 114 (2010): ra23.
 54. V. Labi, C. Woess, S. Tuzlak, et al., "Deregulated Cell Death and Lymphocyte Homeostasis Cause Premature Lethality in Mice Lacking the BH3-only Proteins Bim and Bmf," *Blood* 123, no. 17 (2014): 2652–2662.
 55. K. M. Grebe, R. L. Clarke, and T. A. Potter, "Ligation of CD8 Leads to Apoptosis of Thymocytes That Have Not Undergone Positive Selection," *Proceedings of the National Academy of Sciences* 101, no. 28 (2004): 10410–10415.
 56. E. Y. Zhang, B. L. Parker, and T. M. Yankee, "Gads Regulates the Expansion Phase of CD8+ T Cell-Mediated Immunity," *The Journal of Immunology* 186, no. 8 (2011): 4579–4589.
 57. K. Ruminski, J. Celis-Gutierrez, N. Jarmuzynski, et al., "Mapping the SLP76 Interactome in T Cells Lacking Each of the GRB2-Family Adaptors Reveals Molecular Plasticity of the TCR Signaling Pathway," *Frontiers in immunology* 14 (2023): 1139123.
 58. K. B. Urdahl, D. M. Pardoll, and M. K. Jenkins, "Cyclosporin A Inhibits Positive Selection and Delays Negative Selection in Alpha Beta TCR Transgenic Mice," *Journal of Immunology* 152, no. 6 (1994): 2853–2859.
 59. M. A. Daniels, L. Devine, J. D. Miller, J. M. Moser, A. E. Lukacher, J. D. Altman, et al., "CD8 binding to MHC Class I Molecules Is Influenced by T Cell Maturation and Glycosylation," *Immunity* 2001;15(6):1051–1061.
 60. A. M. Moody, D. Chui, P. A. Reche, J. J. Priatel, J. D. Marth, and E. L. Reinherz, "Developmentally Regulated Glycosylation of the CD8alphabeta Coreceptor Stalk Modulates Ligand Binding," *Cell* 2001;107(4):501–512.
 61. D. M. Berry, S. J. Benn, A. M. Cheng, and C. J. McGlade, "Caspase-Dependent Cleavage of the Hematopoietic Specific Adaptor Protein Gads Alters Signalling From the T Cell Receptor," *Oncogene* 2001;20(10):1203–1211.
 62. T. M. Yankee, K. E. Draves, M. K. Ewings, E. A. Clark, and J. D. Graves, "CD95/Fas Induces Cleavage of the GrpL/Gads Adaptor and Desensitization of Antigen Receptor Signaling," *Proceedings National Academy of Science USA* 2001;98(12):6789–6793.
 63. T. M. Yankee, K. E. Draves, and E. A. Clark, "Expression and Function of the Adaptor Protein Gads in Murine B Cells," *European Journal of Immunology* 2005;35(4):1184–1192.
 64. S. Yamasaki, M. Takase-Utsugi, E. Ishikawa, M. Sakuma, K. Nishida, T. Saito, et al., "Selective Impairment of FcepsilonRI-Mediated Allergic Reaction in Gads-deficient Mice," *International Immunology* 2008;20(10):1289–1297.

Supporting Information

Additional supporting information can be found online in the Supporting Information section.